


The ARIEL mission reference sample

Tiziano Zingales^{1,2}  · Giovanna Tinetti¹ ·
Ignazio Pillitteri² · J r my Leconte³ ·
Giuseppina Micela² · Subhajit Sarkar⁴

Received: 28 April 2017 / Accepted: 9 January 2018 / Published online: 28 February 2018
  The Author(s) 2018. This article is an open access publication

Abstract The ARIEL (Atmospheric Remote-sensing Exoplanet Large-survey) mission concept is one of the three M4 mission candidates selected by the European Space Agency (ESA) for a Phase A study, competing for a launch in 2026. ARIEL has been designed to study the physical and chemical properties of a large and diverse sample of exoplanets and, through those, understand how planets form and evolve in our galaxy. Here we describe the assumptions made to estimate an optimal sample of exoplanets – including already known exoplanets and expected ones yet to be discovered – observable by ARIEL and define a realistic mission scenario. To achieve the mission objectives, the sample should include gaseous and rocky planets with a range of temperatures around stars of different spectral type and metallicity. The current ARIEL design enables the observation of ~1000 planets, covering a broad range of planetary and stellar parameters, during its four year mission lifetime. This nominal list of planets is expected to evolve over the years depending on the new exoplanet discoveries.

Keywords Exoplanets · ARIEL space mission · Planetary population

✉ Tiziano Zingales
tiziano.zingales.15@ucl.ac.uk

¹ University College London, Gower St, Bloomsbury, London WC1E 6BT, UK

² INAF - Osservatorio Astronomico di Palermo, London, UK

³ Laboratoire d’Astrophysique de Bordeaux, CNRS, Universit  de Bordeaux, Bordeaux, Nouvelle-Aquitaine, France

⁴ Cardiff University, Cardiff, UK

1 Introduction

1.1 Mission overview

Today we know over 3700 exoplanets of which more than one third are transiting (<http://exoplanets.eu/>). These include Earths, super-Earths, Neptunes and Giant planets around a variety of stellar types. The Kepler space mission has discovered alone more than 1000 new transiting exoplanets between 2009 and 2015 and more than 3000 still unconfirmed planetary candidates.

The number of known exoplanets is expected to increase in the next decade thanks to current and future space missions (K2, GAIA, TESS, CHEOPS, PLATO) and a long list of ground-based surveys (e.g. HAT-NET, HARPS, WASP, MEarth, NGTS, TRAPPIST, Espresso, Carmenes). These facilities are expected to detect thousands of new transiting exoplanets.

ARIEL (Atmospheric Remote-sensing Exoplanet Large-survey) is one of the three candidate missions selected by the European Space Agency (ESA) for its next medium-class science mission due for launch in 2026. The goal of the ARIEL mission is to investigate the chemical composition of several hundred planets orbiting distant stars in order to address the fundamental questions on how planetary systems form and evolve. Key objective of the mission is to find out whether the chemical composition of exoplanetary atmospheres correlate with basic parameters such as the planetary size, density, temperature, and stellar type and metallicity. During its four-year mission, ARIEL aims at observing a statistically significant sample of exoplanets, ranging from Jupiter- and Neptune-size down to super-Earth and Earth-size in the visible and the infrared with its meter-class telescope. The analysis of ARIEL spectra and photometric data will allow to extract the chemical fingerprints of gases and condensates in the planets' atmospheres, including the elemental composition for the most favorable targets. It will also enable the study of thermal and scattering properties of the atmosphere as the planet orbit around the star.

The main purpose of this paper is to estimate an optimal list of targets observable by ARIEL or a similar mission in the next decade and quantify a realistic mission scenario to be completed in 4 year nominal mission lifetime, including the commissioning phase.

To achieve the mission objectives, the sample should include gaseous and rocky planets with a range of temperatures around stars of different spectral type and metallicity. With this aim, it is necessary to consider both the already known exoplanets and the “expected” ones yet to be discovered. The data collected by Kepler allow to estimate the occurrence rate of exoplanets according to their size and orbital periods. Using this planetary occurrence rate and the number density of stars in the Solar neighbourhood, we can estimate the number of exoplanets expected to exist with a particular size, orbital period range and orbiting a star of a particular spectral type and metallicity. Here we describe the assumptions made to estimate an optimal sample of exoplanets observable by ARIEL and define the Mission Reference Sample (MRS). It is clear that this nominal list of planets will change over the years depending on the new exoplanetary discoveries.

In Section 2 we explain the method used to estimate the number and the parameters of the planetary systems yet to be discovered. All the potential ARIEL targets will be presented in Section 3, where we show all the planets that can be observed individually during the mission lifetime, and out of which we want to select the optimal sample. Section 4 is dedicated to the selection and description of an ARIEL MRS fulfilling the mission requirements, we compare the proposed ARIEL MRS to the sample expected to be discovered by TESS, confirming that TESS could provide a large fraction of the ARIEL targets. A sample including only planets known today is identified. In Section 5 we show a possible MRS which maximises the coverage of the planetary and stellar physical parameters.

1.2 Description of the models

We use the ESA Radiometric Model [13] to estimate the performances of the ARIEL mission given the planetary, stellar and orbital characteristics: namely the stellar type and brightness, the planetary size, mass, equilibrium temperature and atmospheric composition, the orbital period and eccentricity. This tool takes into account the mission instrumental parameters and planetary system characteristics to calculate:

- The SNR (Signal to Noise Ratio) that can be achieved in a single transit;
- The SNR that can be achieved in a single occultation;
- The number of transit/occultation revisits necessary to achieve a specified SNR;
- The total number and types of targets that can be included in the mission lifetime.

In this work, the list of planets considered as input to the radiometric model includes known and simulated exoplanets, as detailed in the following sections. We used the instrument parameters of the ARIEL payload as designed during the phase A study. To increase the efficiency of our simulations we used a Python tool as a wrap of the ESA Radiometric Model, so we could test different mission configurations that fulfil the mission science objectives. The results were validated with ExoSim, a time domain simulator used for the ARIEL space mission, but thanks to its modularity it can be used to study any transit spectroscopy instrument from space or ground. ExoSim has been developed by [11, 15, 16] (see Appendix A).

2 Simulations of planetary systems expected to be discovered in the next decade

2.1 Star count estimate

We used the stellar mass function as obtained from the 10-pc RECONS (REsearch Consortium On Nearby Stars) to estimate the number of stars as a function of the K magnitude. We assume mass-luminosity-K magnitude conversions from [1]. The same procedure was adopted by [14]. The number of main sequence stars with limit K-mag $m_K = 7$ used to infer the number density of stars in the Solar neighbourhood is shown in Table 1.

Table 1 Star counts considering different spectral types with limiting magnitude $m_K = 7$

Mass (M_\odot)	Spectral type	N_* ($K < 7$)
1.25 – 1.09	F6 – F9	5646
1.09 – 0.87	G0 – G8	3356
0.87 – 0.65	K0 – K5	1167
0.65 – 0.41	K7 – M1	386
0.41 – 0.22	M2 – M3	81
0.22 – 0.10	M4 – late M	28

The number density (Table 2) and the number of stars are related through (1):

$$\rho_* = \frac{N_*(K < 7)}{\frac{4}{3}\pi d^3} \quad (1)$$

where the distance d has been calculated in the ARIEL Radiometric Model [13] using the relation between K magnitude m_K and the distance d :

$$m_K = -2.5 \log \frac{R_*^2 S_s(\Delta\lambda)}{d^2 S_0^K(\Delta\lambda)} \quad (2)$$

In (2), R_* is the stellar radius, $S_0^K(\Delta\lambda)$ is the zero point flux for the standard K-band filter profile, $\Delta\lambda$ is the filter band pass given in [4] and $S_s(\Delta\lambda)$ the stellar flux density evaluated over the same bandwidth. We neglect the interstellar absorption since our stars are at a relatively short distance.

2.2 Planetary population and occurrence rate

In this section we briefly review the current knowledge about the occurrence rate of planets, i.e. the average expected number of planets per star. Fressin et al. [5] used the Kepler statistics to publish the planetary occurrence rates around F, G, K main sequence stars ordered by orbital periods and planetary types. An accurate planetary occurrence rate is pivotal to the reliability of the estimate of the existing planets in the Solar neighbourhood. We used the planetary occurrence rate values for F,G,K stars from [5], being the most complete, i.e. covering all planetary types and stars. We have extended the same occurrence rates to M stars but, by doing that, we are

Table 2 Main sequence star densities considering different spectral types with limiting magnitude $m_K = 7$

Density	Star / pc ³
$\rho(\text{F6–F9})$	0.0039
$\rho(\text{G0–G8})$	0.0044
$\rho(\text{K0–K5})$	0.0049
$\rho(\text{K7–M1})$	0.0074
$\rho(\text{M2–M3})$	0.0059
$\rho(\text{M4 – late M})$	0.0118

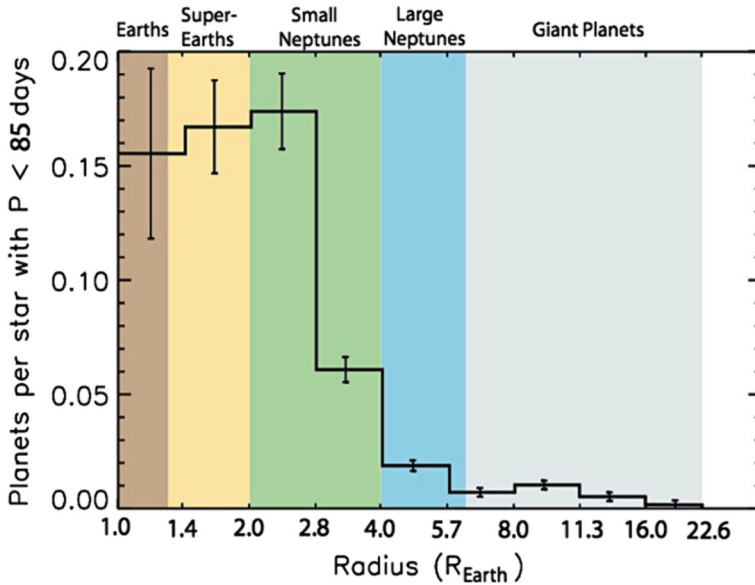


Fig. 1 Average number of planets per star and per size bin with an orbital period shorter than 85 days orbiting around F, G, K stars. The statistics was extracted from the Q1 - Q6 Kepler data [5]

effectively underestimating the number of planets with short period around M dwarfs in our sample (Fig. 1).

Mulders et al. [9] updated the planetary occurrence rate for planets between $0.5R_{\oplus}$ and $4R_{\oplus}$ and orbital period < 50 days, using a more recent list of planets discovered by the Kepler satellite. Figure 2 shows the comparison between [5, 9]. The differences between the two occurrence rates can be up to an order of magnitude. Mulders et al. [8] show that M stars have 3.5 times more small planets ($1.0 - 2.8R_{\oplus}$) than F, G, K stars, but two times fewer Neptune-sized and larger ($> 2.8R_{\oplus}$) planets. The fraction of M-stars considered in our work is only $\sim 7\%$ of the total stellar sample, so we are significantly underestimating the number of small planets around M-dwarfs, which are optimal targets for transit spectroscopy. More recent and complete occurrence rates are expected to be published in the next months. Given the discrepancy between Mulders and Fressin's statistics we expect a substantial improvement in our estimates when the most recent Kepler statistics will become available. The recent papers by Fulton et al. [6] and Mayo et al. [7] confirm this expectations.

Fressin et al. [5] provided the following statistics for different planetary classes:

- Jupiters: $6R_{\oplus} < R_p \leq 22R_{\oplus}$
- Neptunes: $4R_{\oplus} < R_p \leq 6R_{\oplus}$
- Small Neptunes: $2R_{\oplus} < R_p \leq 4R_{\oplus}$
- Super Earths: $1.25R_{\oplus} < R_p \leq 2R_{\oplus}$
- Earths: $0.8R_{\oplus} < R_p \leq 1.25R_{\oplus}$

We adopted a size resolution of $1R_{\oplus}$ in each of these classes.

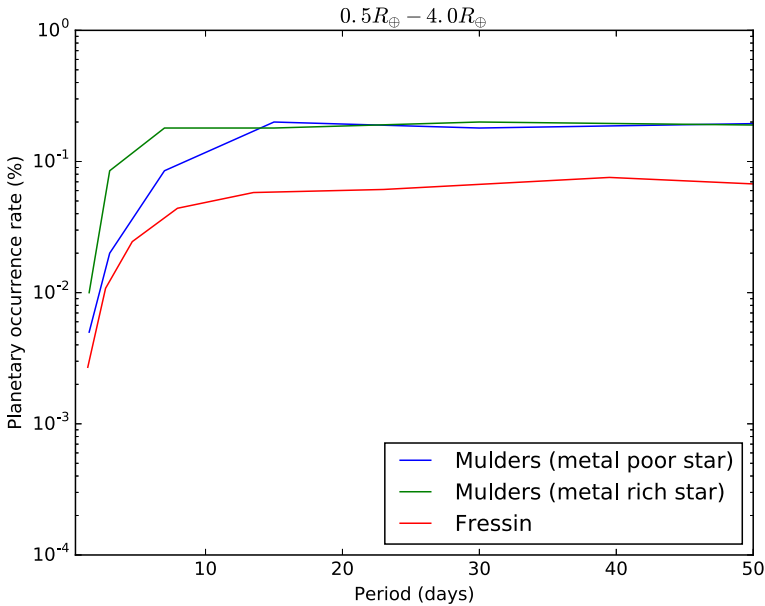


Fig. 2 Comparison of three different distributions estimating the planetary occurrence rate as a function of orbital period for planets between $0.5R_{\oplus}$ and $4R_{\oplus}$. Blue and green lines: results from [9] for two metallicity classes. Red line: results from [5]. The [5] statistics strongly underestimates the occurrence of sub Neptune size planets compared to [9] and other more recent estimates. The reason is the large number of small planets discovered after 2013

The number of planets can be estimated as:

$$N_p = \frac{4}{3}\pi d^3 \rho_* P_{t,p} P_{geom} \tag{3}$$

where d is the radius of a sphere with the Sun at the centre, ρ_* is the number density of the stars, $P_{t,p}$ is the probability of having a t-type planet orbiting with an orbital period p (See Fig. 1). $P_{geom} = R_*/a$ is the geometrical probability of a transit.

We simulated all the transiting planets in the solar neighbourhood up to $m_K = 14$: all these planets described by N_p constitute the “Mission Reference Population”.

To avoid duplications, every time we predicted a planet/star system with the same physical properties of a known one, we replaced it with the known one. In Section 3 we show that in the solar system neighbourhood there are ~ 9500 planets for which the ARIEL science requirements can be achieved in less that 6 transits or eclipses.

The equilibrium temperature (4) of the planet can be estimated assuming the incoming and outgoing radiation at the planetary surface are in equilibrium:

$$T_p = T_* \left(\frac{R_*}{2a} \right)^{\frac{1}{2}} \left(\frac{1 - A}{\epsilon} \right)^{\frac{1}{4}} \tag{4}$$

Here T_* and R_* are the stellar temperature and radius, a the semi-major axis of the orbit, A is the planetary albedo and ϵ is the atmospheric emissivity.

The ARIEL space mission will focus on planets with an orbital period shorter than 50 days. As expected, shorter periods mean shorter semi-major axis and, therefore, from (4), typically warmer temperature.

2.3 Planetary masses and densities

To simulate a realistic planetary population we need to consider a distribution of plausible masses given a planetary radius. The planetary mass controls the surface gravity and therefore the scale height (H) of the atmosphere:

$$H = \frac{k T}{\mu g} \tag{5}$$

Estimating the planetary mass is not a trivial task, given the range of planetary densities observed today. We used a Python tool written by [3] to estimate the mass of all the planets in our simulated sample. Chen and Kipping [3] use the currently known planets to derive the statistical distribution of the mass of a given planet when its radius is known. Thus, except for known systems, for each planet in our simulated sample the mass is randomly drawn following that distribution. In Fig. 3 we show the mass distribution for all the planets in our simulations. Moreover, as a very few planets have a radius larger than $20R_{\oplus}$, we use that radius as an upper limit. There is

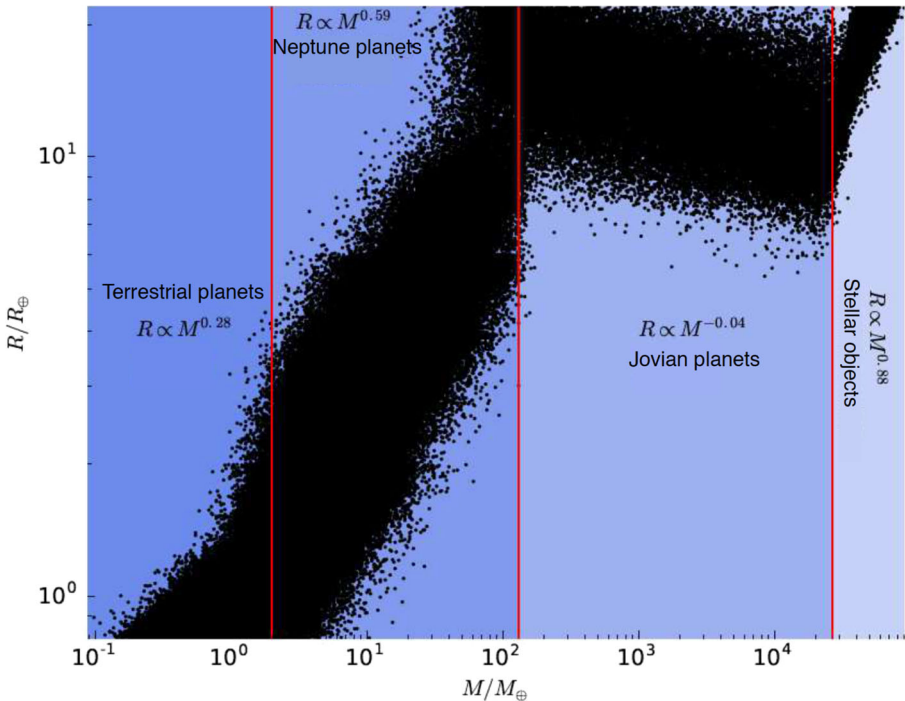


Fig. 3 Mass-Radius distribution for all the simulated planets. The mass-radius relationship has been calculated with the [3] tool

Table 3 Spectral range and spectral resolving power required for the ARIEL photometric and spectroscopic channels

ARIEL spectral coverage		
Channel name	Wavelength (μm)	Resolving power
VisPhot	0.5 – 0.55	Photometer
FGS-1	0.8 – 1.0	Photometer
FGS-2	1.05 – 1.2	Photometer
NIRSpec	1.25 – 1.95	$R \geq 10$
AIRS-Channel #0	1.95 – 3.9	$R \geq 100$
AIRS-Channel #1	3.9 – 7.8	$R \geq 30$

already a well known degeneracy in the $7 - 20R_{\oplus}$ range: objects with a radius within that range can be planets as well as very cool stars. However, this should not be too concerning, as observations have shown that very short-period, low-mass stellar companions are much less frequent than hot giant planets [12].

3 ARIEL science goals and mission reference population

3.1 The 3 tier approach

The ARIEL primary science objectives call for atmospheric spectra or photometric lightcurves of a large and diverse sample of known exoplanets covering a wide range of masses, densities, equilibrium temperatures, orbital properties and host-stars. Other science objectives require, by contrast, the very deep knowledge of a select sub-sample of objects. To maximise the science return of ARIEL and take full advantage of its unique characteristics, a three-tiered approach has been considered, where three different samples are observed at optimised spectral resolutions, wavelength intervals and signal-to-noise ratios. A summary of the three-tiers and observational methods is given below in Tables 3 and 4.

In this section we present the pool of potential targets that could reach the specifications for each tier with a reasonable number of transit/eclipse events. The number of targets for the various Tiers are shown as a function of planetary radius in Figs. 4, 6 and 8 and as a function of effective temperature in 5, 7 and 9. Note that the planets shown in these figures do not represent the final sample, as it would take too

Table 4 Summary of the survey tiers and the observational strategy required to accomplish them. Each tier will use a % of the nominal mission lifetime, as indicated in the left column

ARIEL 3-tiers	
Survey (~37%)	Low spectral resolution observations ($R \geq 10$ across all channels) of a large sample of planets in the Vis-IR, with $\text{SNR} \geq 7$.
Deep (~60%)	Intermediate spectral resolution observations ($R > 50$ in AIRS channel 0 and $R > 15$ in AIRS channel 1) of a sub-sample in the VIS-IR.
Benchmark (~3%)	Very best planets, re-observed multiple time with all techniques. Full spectral resolution.

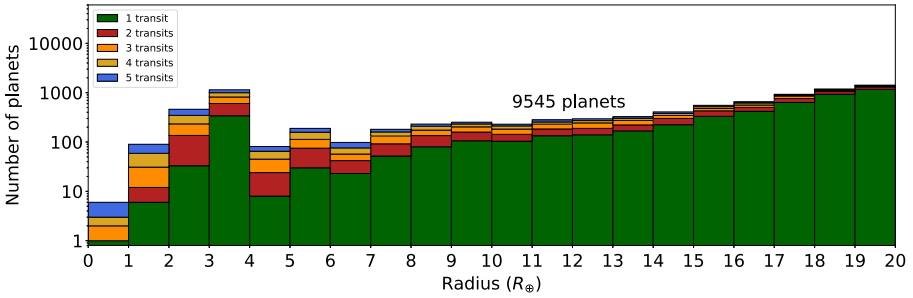


Fig. 4 Complete set of Tier 1 planets from the ARIEL mission reference population. The final list of Tier 1 planets will include an optimal sub-sample. Different colours indicate the number of transits/eclipses needed to reach Tier 1 performances. The planets shown here can achieve the Tier 1 requirements combining the signal of ≤ 5 transits/eclipses

long to observe all of them. They are the pool from which the MRS can be selected to best address the scientific questions summarized below. The fact that the number of potential targets is much larger than the number that can be observed illustrates that ARIEL can choose the final sample among a great variety of observable planets, providing a lot a flexibility.

In Table 3 we show the spectral coverage and the resolving power of the ARIEL photometric and spectroscopic sensors. In Table 4 we report a summary of the three tiers and the observational strategy.

3.2 Key science questions

The key questions and objectives of each tier can be summarised as follows (see Tinetti et al., submitted for further details):

Survey:

- *What fraction of planets are covered by clouds?* – Tier 1 mode is particularly useful for discriminating between planets that are likely to have clear atmospheres, versus those that are so cloudy that no molecular absorption features are visible in transmission. Extremely cloudy planets may be identified simply

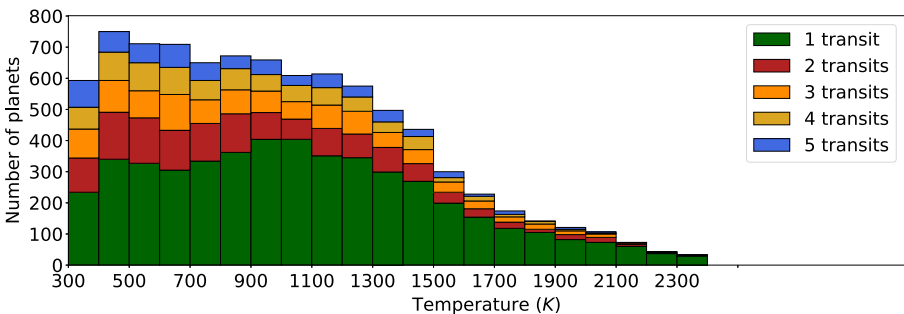


Fig. 5 Temperature distribution for the planets illustrated in Fig. 4

- from low-resolution observations over a broad wavelength range. This preliminary information will therefore allow us to take an informed decision about whether to continue the spectral characterization of the planet at higher spectral resolution, and therefore include or not the planet in the Tier 2 sample.
- *What fraction of small planets have still hydrogen and helium retained from the protoplanetary disk?* – Primordial (primary atmosphere) atmospheres are expected to be mainly made of hydrogen and helium, i.e. the gaseous composition of the protoplanetary nebula. If an atmosphere is made of heavier elements, then the atmosphere has probably evolved (secondary atmosphere). An easy way to distinguish between primordial (hydrogen-rich) and evolved atmospheres (metal-rich), is to examine the transit spectra of the planet: the main atmospheric component will influence the atmospheric scale height, thus changing noticeably the amplitude of the spectral features. This question is essential to understand how super-Earths formed and evolved.
 - *Can we classify planets through colour-colour diagrams or colour-magnitude diagrams?* – Colour-colour or colour-magnitude diagrams are a traditional way of comparing and categorising luminous objects in astronomy. Similarly to the Hertzsprung-Russell diagram, which led to a breakthrough in understanding stellar formation and evolution, the compilation of similar diagrams for exoplanets might lead to similar developments [18].
 - *What is the bulk composition of the terrestrial exoplanets?* – The planetary density may constrain the composition of the planet interior. However this measurement alone may lead to non-unique interpretations [19]. A robust determination of the composition of the upper atmosphere of transiting planets will reveal the extent of compositional segregation between the atmosphere and the interior, removing the degeneracy originating from the uncertainty in the presence and mass of their (inflated?) atmospheres.
 - *What is the energy balance of the planet?* – Eclipse measurements in the optical and infrared can provide the bulk temperature and albedo of the planet, thereby allowing the estimation of the planetary energy balance and whether the planet has an internal heat source or not.

Deep:

A key objective of ARIEL is to understand whether there is a correlation between the chemistry of the planet and basic parameters such as planetary size, density, temperature and stellar type and metallicity. Spectroscopic measurements at higher resolution will allow in particular to measure:

- The main atmospheric component for small planets;
- The chemical abundances of trace gases, which is pivotal to understand the type of chemistry (equilibrium/non equilibrium).
- The atmospheric thermal structure, both vertical and horizontal;
- The cloud properties, i.e. cloud particles size and distribution,
- The elemental composition in gaseous planets. This information can be used to constrain formation scenarios [10].

Benchmark:

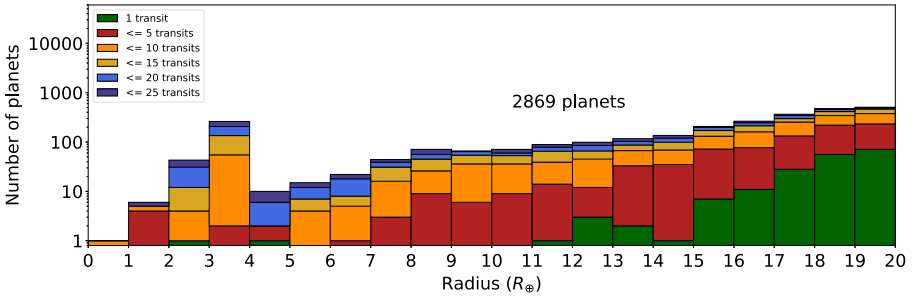


Fig. 6 Planets from the ARIEL mission reference population in the Deep mode (Tier 2) with a small/moderate number of transits/eclipses, divided in size bins. The final list of Tier 2 planets will include an optimal sub-sample. Different colours indicate the number of transits/eclipses needed to reach Tier 2 performances

A fraction of planets around very bright stars will be observed repeatedly through time to obtain:

- A very detailed knowledge of the planetary chemistry and dynamics;
- An understanding of the weather, and the spatial and temporal variability of the atmosphere.

Benchmark planets are the best candidates for phase-curve spectroscopic measurements.

3.3 Target samples

In this section we discuss a number of lists of potential targets for ARIEL: these are expected to evolve until launch and will be updated regularly to include new planet discoveries.

ARIEL Tier 1 (Survey) will analyse a large sample of exoplanets to address science questions where a statistically significant population of objects needs to be observed. ARIEL Tier 1 will also allow a rapid, broad characterisation of planets permitting a more informed selection of Tier 2 and Tier 3 planetary candidates. For

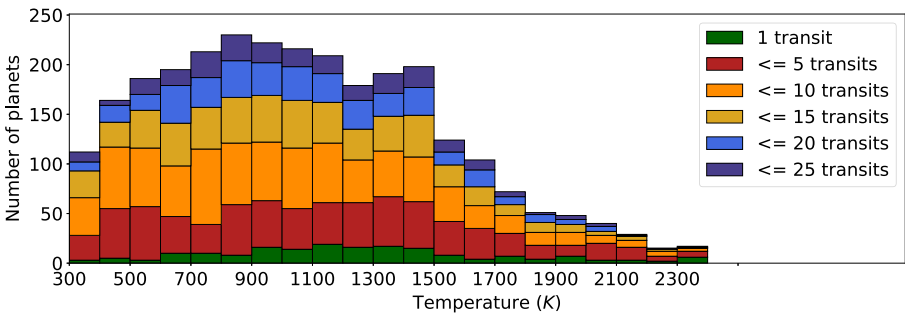


Fig. 7 Temperature distribution for the planets illustrated in Fig. 6

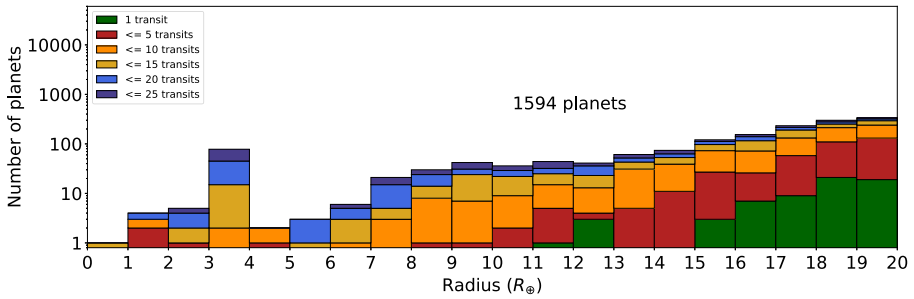


Fig. 8 Number of planets from the mission reference population observable by ARIEL in the Benchmark mode with a < 25 number of transits/eclipses, divided in size bins. Different colours indicate the number of transits/eclipses needed to reach Tier 3 performances

most Tier 1 planetary candidates, Tier 1 performances can be reached between 1 and 2 transits/eclipses. In Figs. 4 and 5 we show that in the solar system neighbourhood there are ~ 9500 observable by ARIEL for which the science requirements can be reached in less than 6 transits or eclipses.

ARIEL Tier 2 (Deep, the core of the mission) will analyse a sub-sample of Tier 1 planets with a higher spectral resolution, allowing an optimal characterisation of the atmospheres, including information on the thermal structure, abundance of trace gases, clouds and elemental composition.

In Figs. 6 and 7 we show the properties of all the planetary candidates that could be studied by ARIEL in the Deep mode with a small/moderate number of transit or eclipse events.

The third ARIEL Tier (Benchmark, the reference planets) will study the best planets (Section 4.3), i.e. the ones orbiting very bright stars which can be studied in full spectral resolution with a relatively small number of transits/eclipses. For the planets observed in benchmark mode in 1 or 2 events, it is possible to study the spatial and temporal variability (i.e. study the weather and evaluate its impact when observations are averaged over time). In Figs. 8 and 9 we show the properties of the Tier 3 planetary candidates.

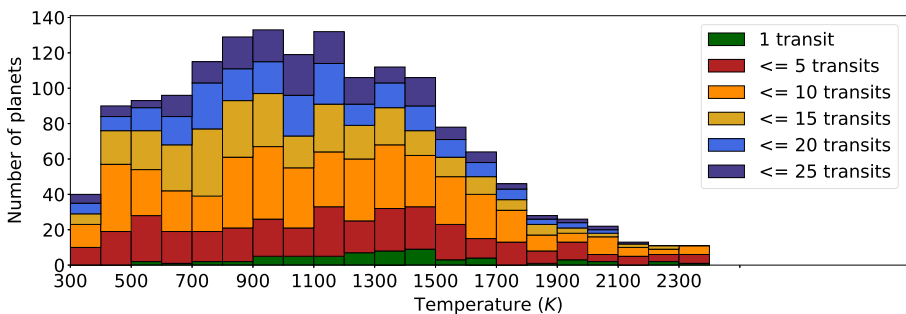


Fig. 9 Temperature distribution for the planets illustrated in Fig. 8

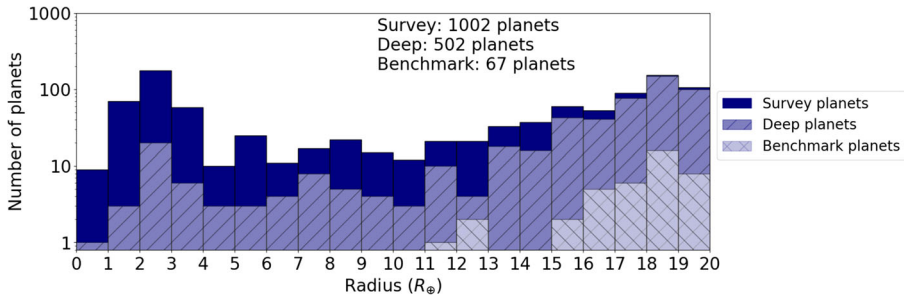


Fig. 10 Overview of the ARIEL MRS, comparing the number of planets observable in the three tiers during the mission lifetime

4 A possible scenario for the ARIEL space mission

In Section 3 we presented a comprehensive list of planet candidates which could be observed with the ARIEL space mission. Here we discuss possible optimisations of the Mission Reference Sample, which ideally should include a large and diverse sample of planets, have the right balance among the three Tiers and, most importantly, must be completed during the nominal mission lifetime (4 years including the commissioning phase).

In Fig. 10 we show a possible MRS with all the three tiers nested together. This MRS is optimised to yield the maximum number of targets, taking into account the nominal mission lifetime. It has been built starting from all the targets feasible within one transit/eclipse, and adding all the targets that can be done within 2, 3, 4 and so on transits/eclipses in ascending order. This is just one of the possible configurations for the MRS, and one would expect the ARIEL MRS to evolve in response of new exoplanetary discoveries in the next decade.

4.1 MRS tier 1: survey

Our simulations indicate that the current ARIEL design as presented at the end of the Phase A study, allows to observe 1002 planets in Tier 1. All the planets can be

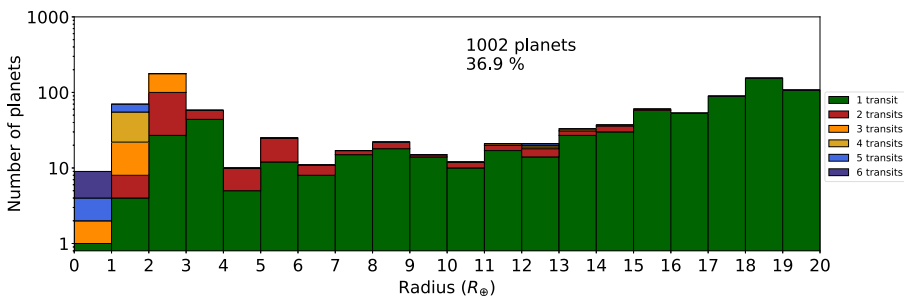


Fig. 11 ARIEL MRS Tier 1 planets organised in size-bins. Different colours indicate the number of transits/eclipses needed to reach Tier 1 performances

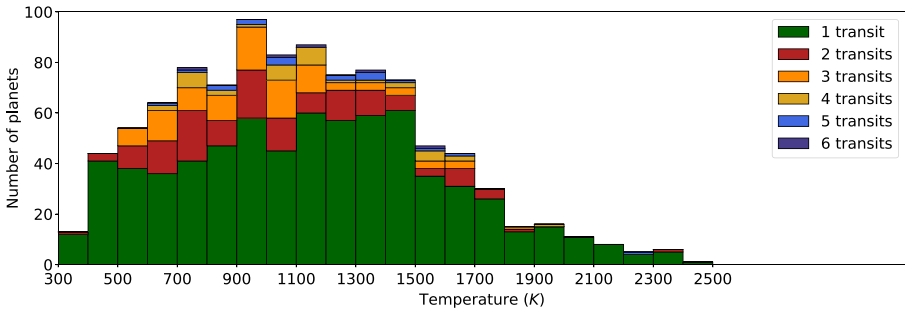


Fig. 12 ARIEL MRS Tier 1 planets organised in temperature-bins. Different colours indicate the number of transits/eclipses needed to reach Tier 1 performances

observed during 37% of the mission lifetime. Most giant planets and Neptunes fulfil the Tier 1 science objectives in 1 transit/eclipse, the smaller planets require up to 6 events (Figs. 11 and 12). Figures. 13 and 14 illustrate how the 1002 planets are distributed in terms of planetary size, temperature, density and stellar type.

4.2 MRS tier 2: deep

The Deep is the core of the mission. Our simulations indicate that the current ARIEL design as presented at the end of the Phase A study, allows to observe ~ 500 planets in Tier 2 assuming 60% of the mission lifetime. Most Gaseous planets fulfil the Tier 2 science objectives in less than five transits/eclipses, the small planets require up to twenty events (Figs. 15 and 16). Figures 17 and 18 illustrate how the 500 planets are distributed in terms of planetary size, temperature, density and stellar type.

We included a variety of planets from cold (300 K) to very hot (2500 K) as shown in Fig. 16. We scheduled also ~ 50 planets that will be studied with both transit and eclipse methods, indicated by stripes in Fig. 15). These are the best candidates for

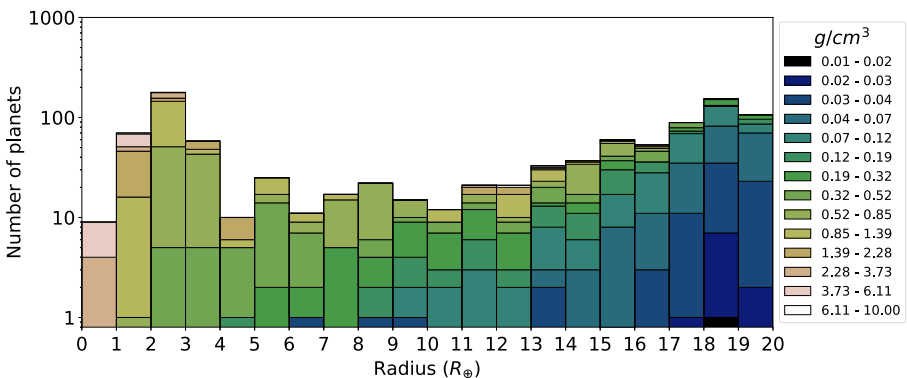


Fig. 13 ARIEL MRS Tier 1 planets organised in size-bins. Different colours indicate differences in the simulated planetary densities

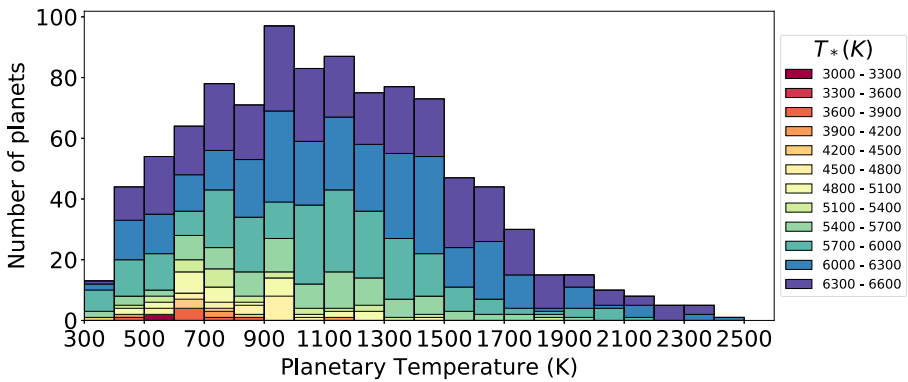


Fig. 14 ARIEL MRS Tier 1 planets organised in temperature-bins. Different colours indicate differences in the simulated stellar temperatures

phase-curves observations, which can be included at the expenses of the number of Tier 2 planets observed.

4.3 MRS tier 3: benchmark

In the current MRS, we have selected as Tier 3, 67 gaseous planets for weather studies. Figure 19 shows the temperature distribution covered by the Tier 3 sample. Only 3% of the mission lifetime is required to achieve the Tier 3 science objectives for this sample.

4.4 Compliance with TESS expected yields

The Transiting Exoplanet Survey Satellite (TESS) is expected to provide a large fraction of the targets observable by ARIEL. The numbers of targets envisioned in the sample presented here are perfectly in line with the expected yield from The Transiting Exoplanet Survey Satellite (TESS), as shown in Fig. 20 where we compare the expected TESS discoveries and the ARIEL MRS. We see that the ARIEL MRS is

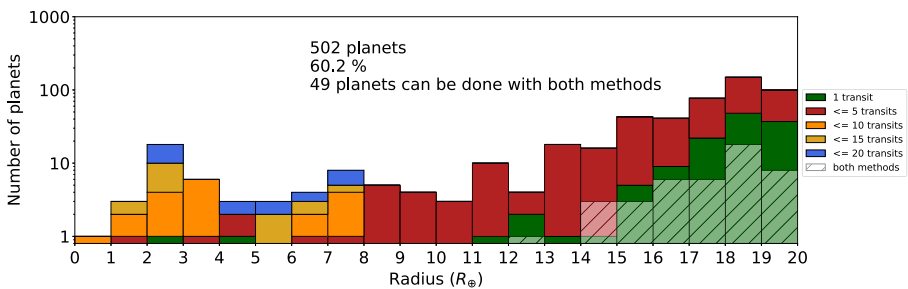


Fig. 15 ARIEL MRS Tier 2 planets organised in size-bins. Different colours indicate the number of transits/eclipses needed to reach Tier 2 performances. Stripes indicate planets that will be studied both transit and eclipse methods

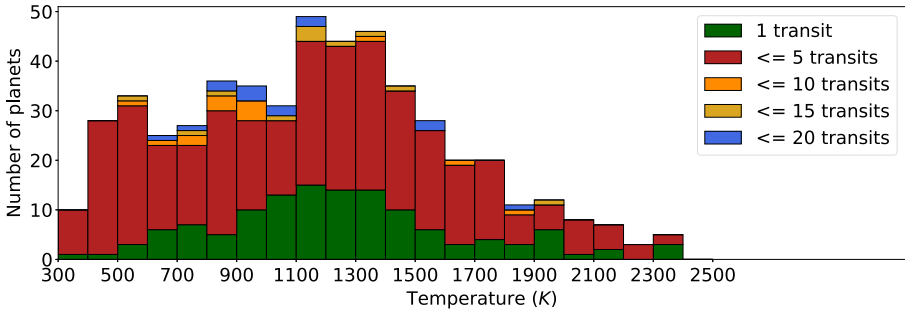


Fig. 16 ARIEL MRS Tier 2 planets organised in temperature-bins. Different colours indicate the number of transits/eclipses needed to reach Tier 2 performances

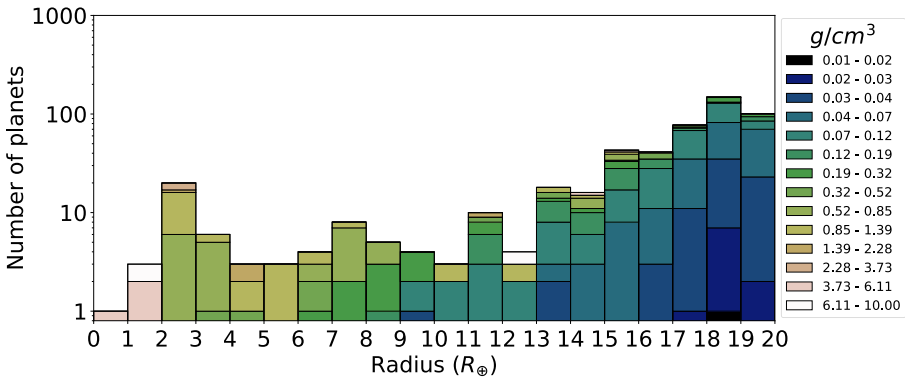


Fig. 17 ARIEL MRS Tier 2 planets organised in size-bins. Different colours indicate differences in the simulated planetary densities

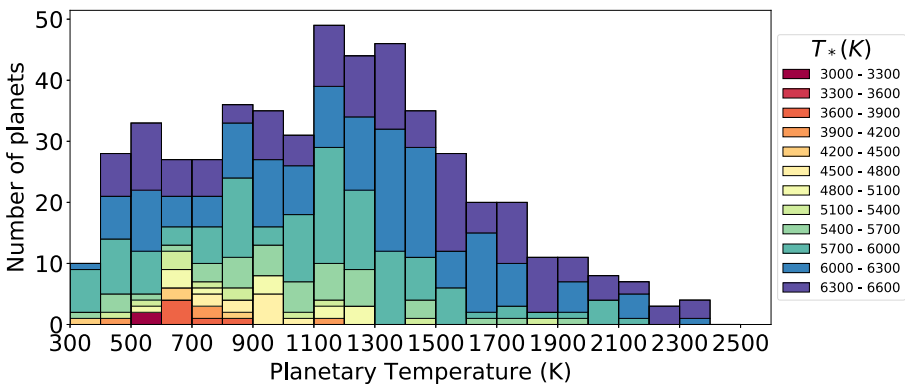


Fig. 18 ARIEL MRS Tier 2 planets organised in temperature-bins. Different colours indicate differences in the simulated stellar temperatures

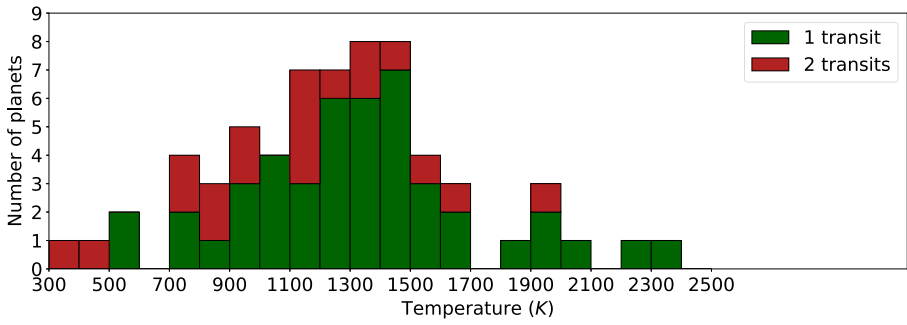


Fig. 19 Temperature distribution of the planets observable by ARIEL in the Benchmark

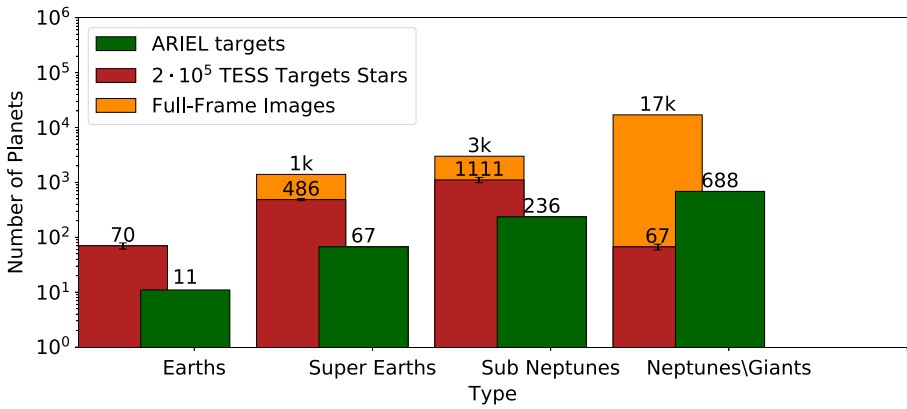


Fig. 20 Comparison between the TESS targets [17] and the ARIEL MRS (green bars)

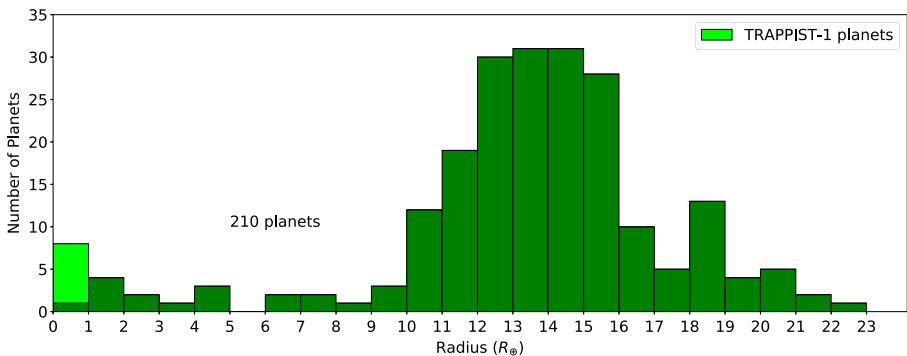


Fig. 21 ARIEL MRS with currently available planets radius distribution

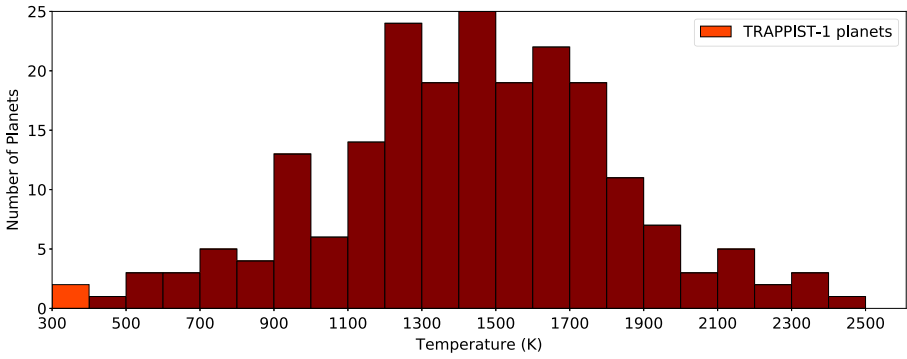


Fig. 22 ARIEL MRS with currently available planets temperature distribution

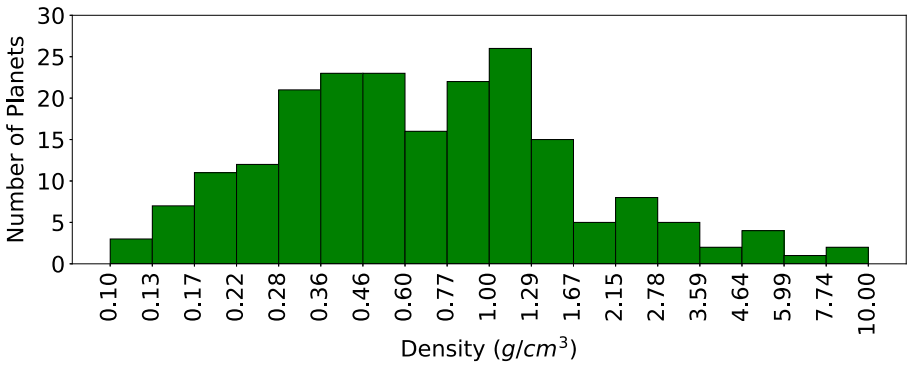


Fig. 23 ARIEL MRS with currently available planets density distribution

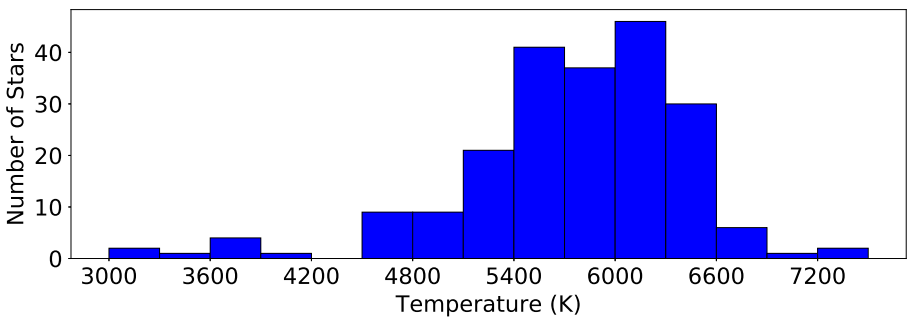


Fig. 24 Temperature distribution of the stellar hosts for the planets shown in Fig. 21

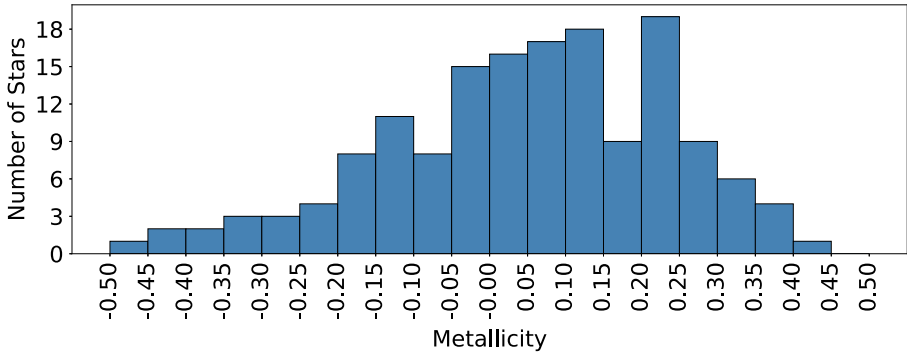


Fig. 25 Metallicity distribution of the stellar hosts for the planets shown in Fig. 21

well within the TESS sample [17]. The success of the TESS mission will allow the characterisation of hundreds of planets by ARIEL.

4.5 ARIEL MRS with currently known targets

In February 2017 ~210 transiting planets fulfill the ARIEL previous criteria. It means that, even if ARIEL were launched tomorrow, it would observe at least 210 relevant

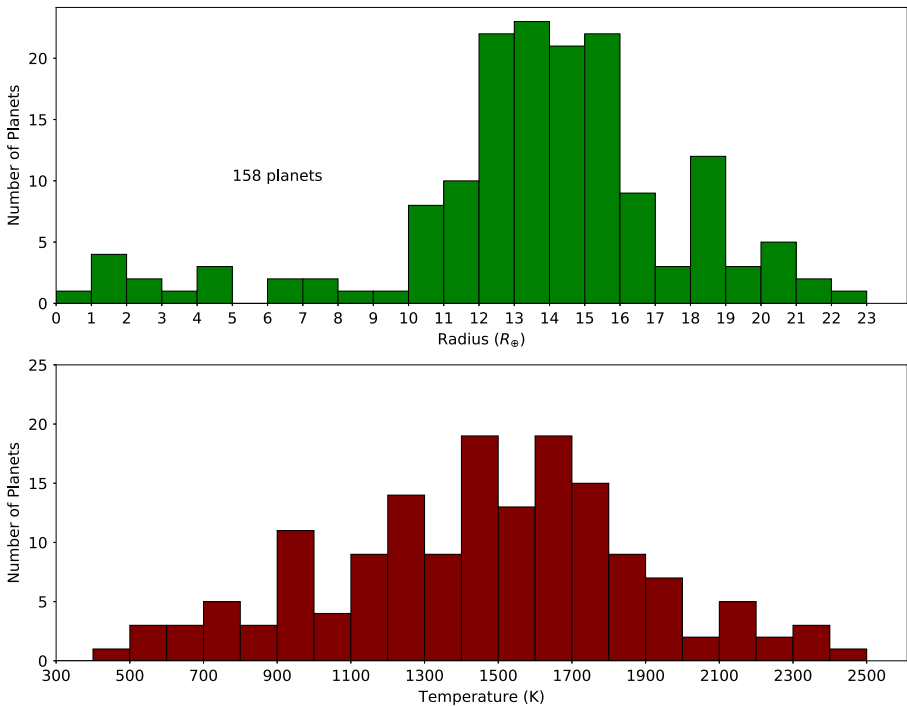


Fig. 26 Planets known today and observable by ARIEL in Deep mode, distributed in size-bins (top) and temperature bins (bottom) – 158 planets

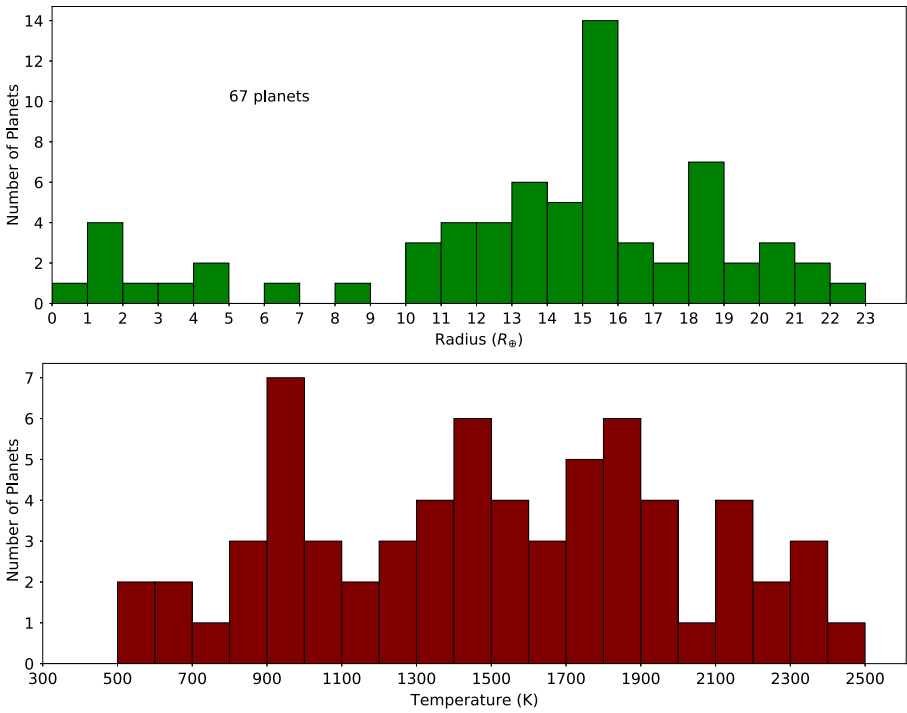


Fig. 27 Planets known today and observable by ARIEL in Benchmark mode, distributed size-bins (top) and temperature bins (bottom) – 67 planets

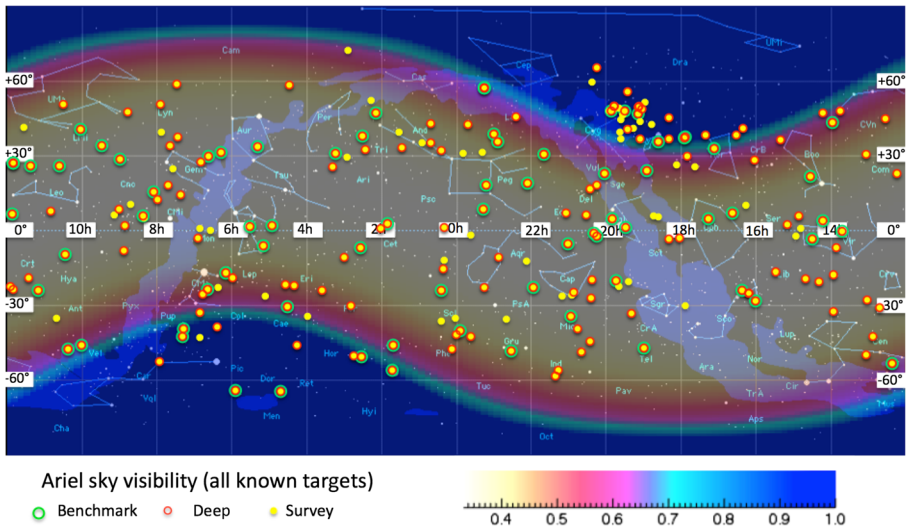


Fig. 28 A plot illustrating the fraction of the year for which a given location in the sky (in equatorial coordinates) is visible to ARIEL, as seen from a representative operational orbit of ARIEL at L2. Yellow dots: planets observed in Tier 1. Red dots: planets observed in Tier 2. Green dots: planets observed in Tier 3. (Marc Ollivier, private communication)

targets. Using the planets known today, we could organise the MRS into the following three tiers:

- Survey: 210 planets using 30% of the mission lifetime (Fig. 21);
- Deep: 158 planets using 60% of the mission lifetime (Fig. 26);
- Benchmark: 67 planets using 10% of the mission lifetime (Fig. 27).

In Figs. 21, 22 and 23 we show the key physical parameters of the known planets defining the current observable MRS current MRS. In Figs. 24 and 25 we show the properties of the stellar hosts. A possible deep and benchmark mode configuration is shown, respectively, in Figs. 26 and 27. As mentioned previously, the number of known planets is expected to increase dramatically in the future.

Pictorial representation (M. Ollivier, private comm.) of the known planets sky coordinates and their sky visibility all over the year is given in Fig. 28. It shows that

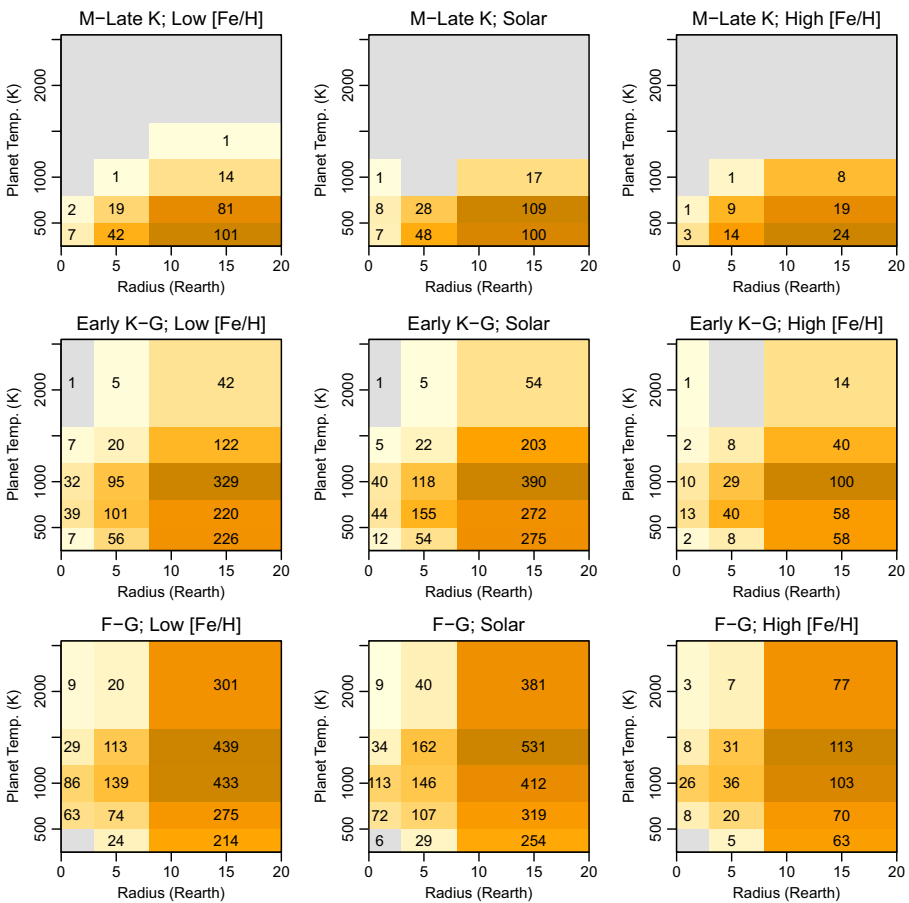


Fig. 29 Distribution of the 9545 planets in the 4D space of T_{eff} , $[\text{Fe}/\text{H}]$, R_{pl} , T_{pl} . Above each panels we indicate the spectral type and metallicity. The numbers in each cell are the numbers of planets with the corresponding properties. The colour scale indicates more populated cells (darker orange/brown). Grey cells without any number indicate no objects

objects far away from the ecliptic plane will be visible longer than the planet close to this plane.

5 MRS optimisation for stellar hosts

In this section we show another possible selection of the Tier 1 sample that maximises also the diversity of stellar hosts, additionally to other planet parameters. In particular, the stellar metallicity is expected to play an important role in the planet formation process and type of chemistry of the planet [20]. ARIEL will also collect important data to test the possible correlations between stellar metallicity and planetary characteristics.

5.1 Method

We will limit our analysis to those systems which can be studied in up to six visits for each planet (either a transit or an occultation).

We chose four physical quantities that define a 4D space to distribute the ARIEL targets. The quantities are: stellar effective temperature (T_{eff}), metallicity ($[\text{Fe}/\text{H}]$), planetary radius (R_{pl}) and planetary theoretical equilibrium temperature (T_{pl}) (Fig. 29). For the metallicity we use the values observed in the solar neighbourhood and reported by [2]. We adopt three bins for stellar T_{eff} , $[\text{Fe}/\text{H}]$ and planetary R_{pl} , while for the T_{pl} we use five bins, as detailed in Table 5. The three T_{eff} bins correspond approximately to the ranges of spectral types M-Late / K stars, Early K-G stars and F-G stars, respectively, as indicated in the labels in Figs. 30, 31 and 32. Analogously, we separated the sample in low metallicity, solar metallicity and high metallicity, according to individual temperature values. The binning into 3 intervals of T_{eff} , $[\text{Fe}/\text{H}]$ and R_{pl} is a reasonable trade-off between a detailed representation of the sample and a simple visualization of the richness and diversity of the physical configurations of the sample. We inferred from [2] that the metallicities of stars in the solar neighbourhood are consistent with a normal distribution with mean -0.1 and standard deviation $\text{sd}=0.2$. Using such model distribution we simulated the values of $[\text{Fe}/\text{H}]$ for each star in the ARIEL sample.

Table 5 Bins of T_{eff} , $[\text{Fe}/\text{H}]$, R_{pl} , T_{pl} defining the 4D parameter space

Stellar Temp.: T_{eff}	$3000 < T(\text{K}) < 4100$	$4100 < T(\text{K}) < 5800$	$T > 5800\text{K}$
Labels	M-Late K	Early K-G	F-G
Metallicity: $[\text{Fe}/\text{H}]$	$[\text{Fe}/\text{H}] < -0.15$	$-0.15 < [\text{Fe}/\text{H}] < 0.15$	$[\text{Fe}/\text{H}] > 0.15$
Labels	Low $[\text{Fe}/\text{H}]$	Solar	High $[\text{Fe}/\text{H}]$
Planet Radius: R_{pl}	$R_{\text{pl}} < 3R_{\oplus}$	$3 < R_{\oplus} < 8$	$R_{\text{pl}} > 8R_{\oplus}$
Labels	Earths/ Super Earths	Neptunes	Jupiters
Planet Temp.: T_{pl}	contiguous bins: [250, 500, 800, 1200, 1600, 2600] K		

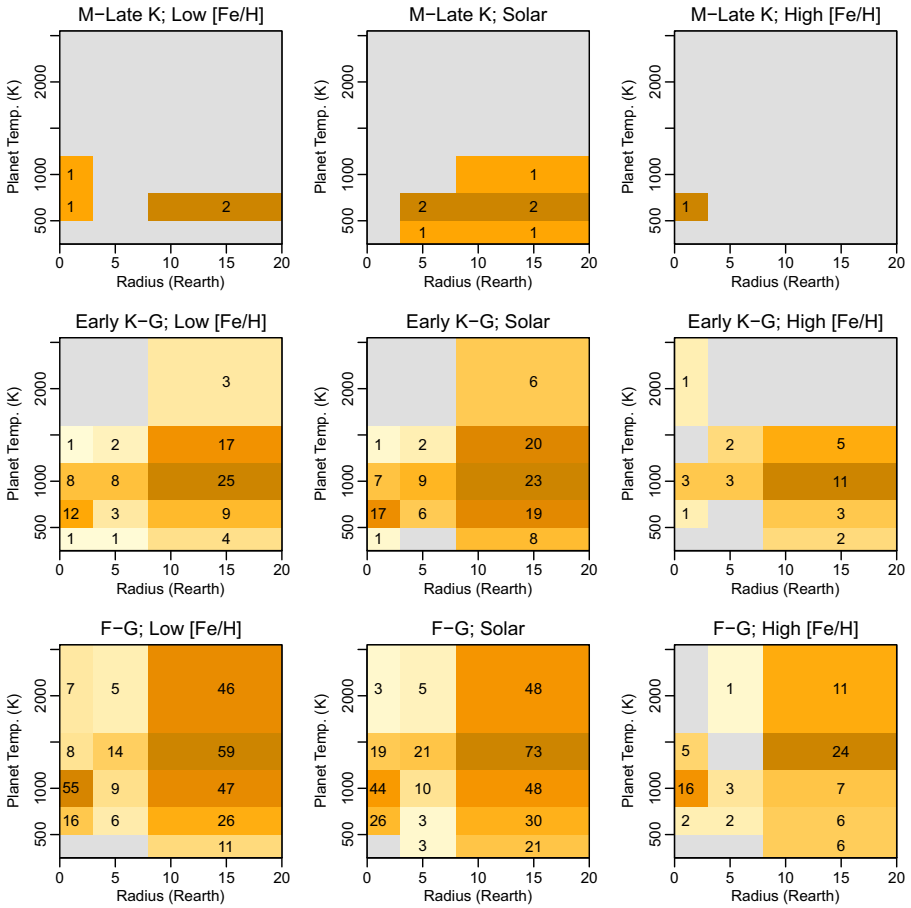


Fig. 30 Same as Fig. 29 1002 planets of the Mission Reference Sample

The 4D space of T_{eff} , $[\text{Fe}/\text{H}]$, R_{pl} and T_{pl} is composed by a total of $3 \times 3 \times 3 \times 5 = 135$ cells. We assume that 10 systems are sufficiently reliable to determine the properties of the atmospheres of planets in each cell.

5.2 Results

The population of 9545 planets is distributed in the 4-D bins as in Fig. 29.

From this distribution we selected 1002 exoplanets, requiring altogether 1538 satellite visits. These 1002 planets are distributed in the 4D space as shown in Fig. 30. The 3×3 panel grid distributes the sample along the 3 spectral types and the metallicity ranges reported in Table 5. Each panel is a matrix with planetary radii along x-axis and (calculated) equilibrium temperatures along y-axis, as specified in Table 5 and discussed above. The numbers in each box identify the numbers of systems with the corresponding R_{pl} , T_{pl} , spectral type, and $[\text{Fe}/\text{H}]$ values.

The 1002 systems in Fig. 30 tend to populate the cells corresponding to F-G-early and K stars orbited by Neptunes/Jupiters size planets (with a number of planets per cell $N > 20$), as these systems are the easiest to be observed with high signal to noise and, on average, with one or two visits. At the same time, planets around M or late K stars are much less represented in this distribution, especially planets smaller than Neptune. This issue was identified in the previous sections as a result of extending the occurrence rate for F, G, K to M stars and it can be addressed by prioritising these targets over the rest of the population. We selected 908 planets and, in particular, 594 of them require only 1 visit (65.4%), 151 planets require 2 visits (16.6%), 83 planets require 3 visits (9.1%), 41 planets require 4 visits (4.5%), and 39 planets require 5 visits (4.4%). The corrected sample is shown in Fig. 31, where now $\sim 19\%$ of the population are Earths/Super Earth or Neptunes around M or K stars observable with less than 6 visits.

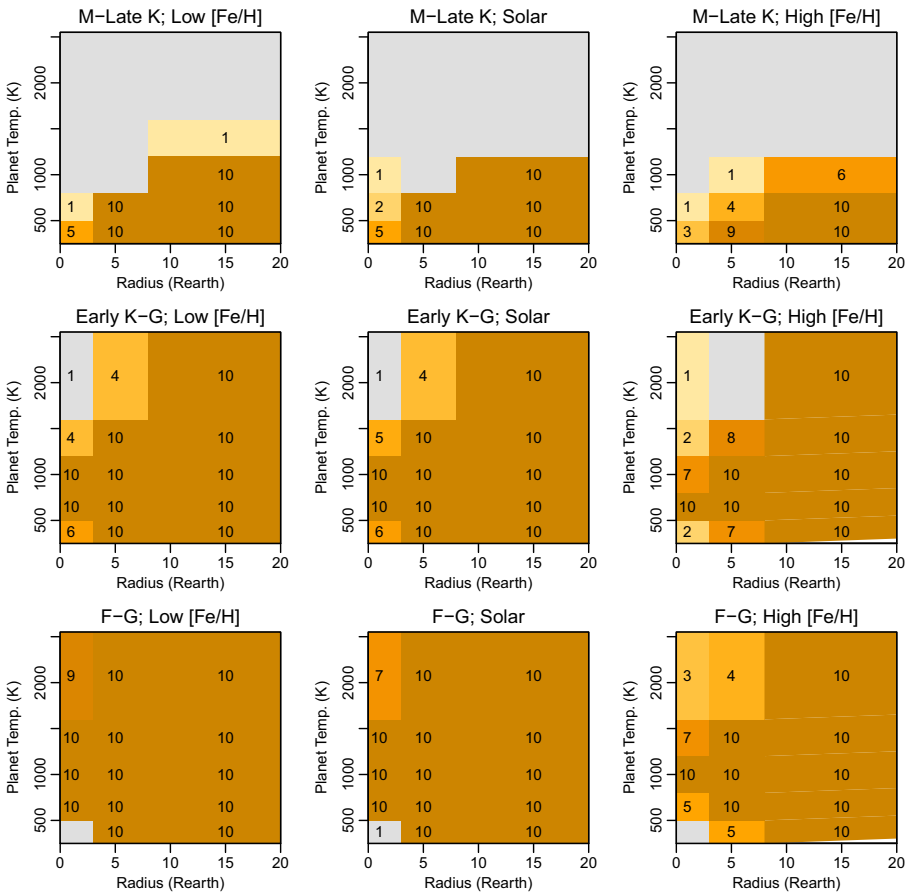


Fig. 31 Same as Fig. 30 for the selected sample of 908 known and simulated planetary systems. They have been selected by filling each cell with up to 10 objects and for a budget of total satellite visits of about 1500

Assuming a total number of visits as in the 1002 planets configuration (approximately 1500 visits), we fixed the maximum number of systems (10 planets in our choice) in each 4D space cell. This choice implies that any additional targets in an “already full” cell will be discarded. In this way we can include planets in the empty or poorly populated parts of the parameter space. The goal is to verify that we can cover with enough statistics most of the 4D parameter space. The distribution of systems selected with such criteria is shown in Fig. 31. Compared to Fig. 30, we see that we can efficiently cover most of the 4D space in planetary sizes, planetary temperatures, host temperatures and metallicities, apart from those combination of parameters corresponding to not physical or rare systems (e.g., very hot planets around very cool stars). Our selection is composed by 908 unique planets requiring a total of 1504 visits. Among already known systems, 92 of the initial 211 systems are in this new list. This selection is not unique, and depends on our choices, but our exercise shows that we have great freedom on the final choice on how to spend ARIEL observing time, as it can be easily tuned on specific needs.

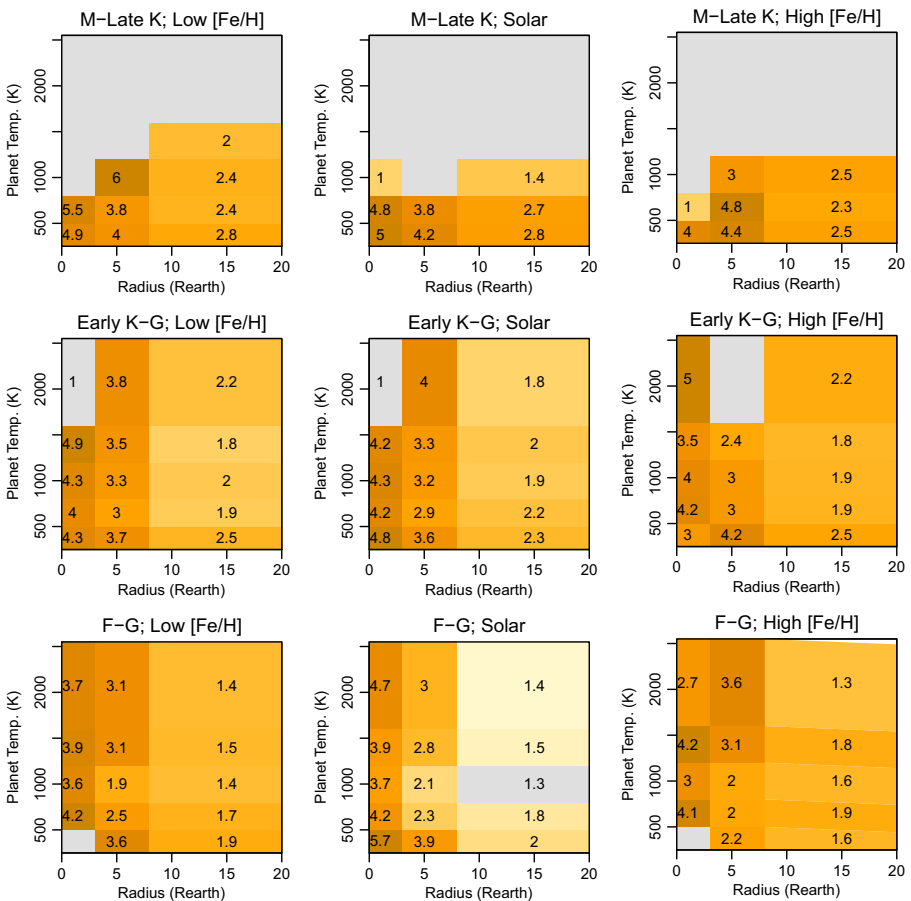


Fig. 32 Average number of visits required for the sample selected in Fig. 31. The binning is as in Figs. 30 to 31

Figure 32 shows the average number of visits required to cover each cell of the 4D space. The number of visits needed for Jupiters and Neptunes is, typically, one or two, while Earths/Super Earths require from 3 to 5 visits each. To summarise, out of the 908 planets in our selection there are 594 planets requiring only 1 visit (65.4%), 151 planets requiring 2 visits (16.6%), 83 planets requiring 3 visits (9.1%), 41 planets requiring 4 visits (4.5%), and 39 planets requiring 5 visits (4.4%).

As a final comment, we have verified that, by increasing the maximum number of systems per 4D cell while keeping fixed the total number of visits to ~ 1500 , we obtain that the number of observed planets increases (for example assuming $N=15$ as maximum systems per cell, we can observe up to 1000 systems), but at the same time the 4D cells of systems with cold/warm Earths/Super Earths would tend to be left empty and thus unexplored. This exercise shows the degree of flexibility offered by ARIEL in the choice of the target sample.

6 Conclusions

In this paper we demonstrated that the current ARIEL design enables the observation of 900–1000 planets during its four-year lifetime, depending on the physical parameters of the planet/star systems which one wants to optimise. The optimal sample of targets fulfils all the science objectives of the mission. While we currently know only ~ 200 transiting exoplanets which could be part of the mission reference sample, new space missions and ground-based observatories are expected to discover thousands of new planets in the next decade. NASA-TESS alone is expected to deliver most ARIEL targets.

Acknowledgements T. Z. is supported by the European Research Council ERC projects *ExoLights* (617119) and from INAF through the “Progetti Premiali” funding scheme of the Italian Ministry of Education, University, and Research. I.P and G.M. are supported by Ariel ASI-INAF agreement No. 2015-038-R.0. We thank Enzo Pascale and Ludovig Puig for their help in setting up the ESA’s Radiometric model.

Open Access This article is distributed under the terms of the Creative Commons Attribution 4.0 International License (<http://creativecommons.org/licenses/by/4.0/>), which permits unrestricted use, distribution, and reproduction in any medium, provided you give appropriate credit to the original author(s) and the source, provide a link to the Creative Commons license, and indicate if changes were made.

Appendix A: ESA Radiometric Model validation with ExoSim

We compare the out-of-transit signal and noise from ESA Radiometric Model (ERM) with that from ExoSim. An early version of ARIEL with a grating design was used for the instrument model in each. We model 55 Cancri and GJ 1214 with the same PHOENIX spectra in each simulator and include only photon noise and the noise floor, $N_{min}(\lambda)$, which is dominated by dark current noise. All the calculations are done per unit time and per spectral bin ($R = 30$ in Ch1 and $R = 100$ in Ch0). The noise variance was compared assuming an aperture mask on the final images, and the

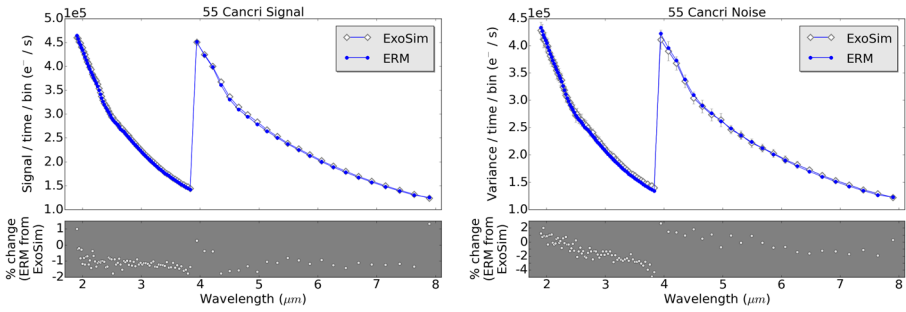


Fig. 33 Comparison between the out-of-transit signal (left) and noise (right) simulated by ExoSim (white points) and the ESA Radiometric Model (blue points) for the star 55 Cancri. Subplots show the percent difference of the ERM from ExoSim

noiseless signal per unit time was compared assuming no aperture. In the ERM, we use the following expression for N_{min} giving the noise variance:

$$N_{min}(\lambda) = \frac{2.44 f \lambda^2}{m R \Delta_{pix}^2} I_{dc} \tag{6}$$

where I_{dc} is the dark current per pixel, m is the reciprocal linear dispersion of the spectrum in μm wavelength per μm distance, R is the spectral resolving power and Δ_{pix} is the pixel pitch. The ExoSim noise variance results are the mean results from 50 simulations, with the standard deviations shown as error bars in the following figures. For 55 Cancri e case (Fig. 33), over all wavelength bins, the ERM signal is always within 2% of ExoSim, and the averaged noise variance within 5% of the ERM. In 94% of the bins, the ERM noise variance is within the standard deviation from ExoSim.

For GJ 1214 (Fig. 34), the ERM signal is within 4% of ExoSim over all bins and the averaged noise variance within 6% of ExoSim over all bins. The ERM noise variance is always within the standard deviation from ExoSim over all bins.

There is therefore good agreement between the two simulators.

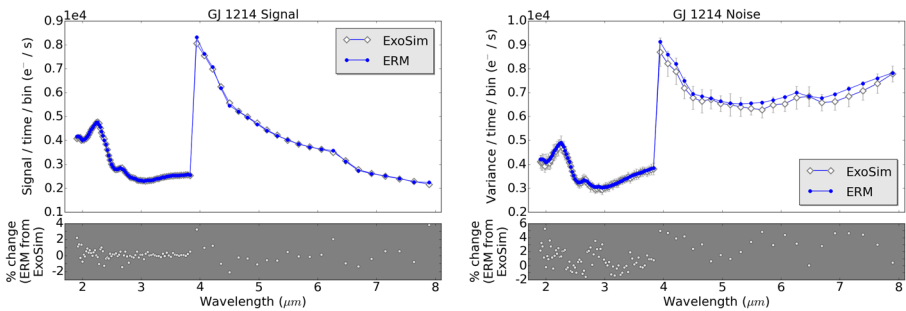


Fig. 34 Comparison between the out-of-transit signal (left) and noise (right) simulated by ExoSim (white points) and the ESA Radiometric Model (blue points) for the star GJ 1214. Subplots show the percent difference of the ERM from ExoSim

Appendix B: Known planets observable by ARIEL

Table 6 List of known planets observable by ARIEL. The former to last column represents the number of transits/eclipses necessary to fulfil the ARIEL Tier 1 goals

#	Planet	Planetary properties				Stellar properties		Observation	
		R (R_{\oplus})	M (M_{\oplus})	P (days)	T (K)	R (R_{\odot})	T (K)	#	Type
1	55 Cnc e	1.88	8.07	0.74	1891	0.95	5196	1	transit
2	EPIC 204129699 b	15.47	563.97	1.26	1473	0.91	5280	1	transit
3	WASP-52 b	13.94	146.24	1.75	1267	0.87	5000	1	transit
4	HD 189733 A b	12.49	361.78	2.22	1180	0.80	4980	1	transit
5	WASP-77 A b	13.28	559.52	1.36	1762	1.00	5500	1	transit
6	WASP-85 A b	16.24	387.85	2.66	1341	1.04	5685	1	transit
7	WASP-33 b	15.78	1459.19	1.22	2541	1.50	7200	1	occultation
8	WASP-19 b	15.21	371.32	0.79	1998	0.97	5500	1	occultation
9	WASP-95 b	13.28	359.23	2.18	1521	1.11	5630	1	transit
10	WASP-121 b	19.83	376.08	1.27	2295	1.35	6459	1	transit
11	WASP-12 b	19.05	446.34	1.09	2399	1.35	6118	1	occultation
12	WASP-35 b	14.48	228.89	3.16	1414	1.07	5990	1	transit
13	HAT-P-30 b	14.70	226.03	2.81	1594	1.24	6304	1	transit
14	WASP-108 b	14.09	283.57	2.68	1558	1.17	6000	2	transit
15	HD 209458 b	15.14	226.99	3.52	1401	1.15	6075	1	transit
16	WASP-122 b	21.64	436.17	1.71	1900	1.40	5720	1	transit
17	WASP-2 A b	12.26	290.57	2.15	1276	0.89	5255	2	transit
18	HAT-P-32 b	22.35	299.15	2.15	1850	1.18	6207	1	transit
19	WASP-43 b	11.37	646.62	0.81	1403	0.72	4520	1	occultation
20	WASP-123 b	14.56	292.47	2.98	1477	1.21	5740	1	transit
21	WASP-101 b	15.47	158.95	3.59	1518	1.34	6400	1	transit
22	WASP-74 b	17.12	302.01	2.14	1872	1.48	5990	1	transit
23	WASP-76 b	20.08	292.47	1.81	2125	1.46	6250	1	transit
24	WASP-1 b	16.27	271.49	2.52	1777	1.24	6160	1	occultation
25	KELT-10 b	15.35	215.86	4.17	1340	1.11	5948	1	transit
26	KELT-3 b	14.90	464.78	2.70	1774	1.28	6304	1	transit
27	WASP-62 b	15.25	181.21	4.41	1389	1.25	6230	1	transit
28	HD 149026 b	7.88	113.17	2.88	1699	1.30	6147	1	transit
29	WASP-97 b	12.40	419.64	2.07	1500	1.12	5640	2	occultation
30	WASP-94 A b	18.87	143.69	3.95	1464	1.29	6170	1	transit
31	HAT-P-8 b	14.50	405.33	3.08	1687	1.19	6200	1	occultation
32	WASP-54 b	18.14	202.19	3.69	1531	1.15	6100	1	transit
33	WASP-109 b	15.83	289.30	3.32	1729	0.91	6520	1	transit
34	HAT-P-41 b	18.49	254.33	2.69	1886	1.42	6390	1	transit
35	HAT-P-13 b	14.05	270.22	2.92	1600	1.22	5638	1	transit
36	KELT-15 b	15.83	289.30	3.33	1500	1.18	6003	2	transit
37	KELT-7 b	16.82	406.92	2.73	1996	1.53	6789	1	transit

Table 6 (continued)

#	Planet	Planetary properties				Stellar properties		Observation	
		R (R_{\oplus})	M (M_{\oplus})	P (days)	T (K)	R (R_{\odot})	T (K)	#	Type
38	HAT-P-6 b	14.59	336.03	3.85	1629	1.29	6570	2	transit
39	WASP-49 b	12.24	120.17	2.78	1334	0.94	5600	1	transit
40	WASP-15 b	15.67	172.31	3.75	1609	1.18	6300	1	transit
41	WASP-79 b	18.65	286.12	3.66	1709	1.56	6600	1	transit
42	KELT-4A b	18.64	286.75	2.99	1779	1.20	6206	1	transit
43	WASP-17 b	21.85	154.50	3.74	1725	1.31	6650	1	transit
44	WASP-3 b	15.96	654.89	1.85	1933	1.24	6400	1	occultation
45	WASP-7 b	14.59	305.19	4.95	1448	1.28	6400	1	transit
46	KELT-8 b	20.41	275.63	3.24	1633	1.21	5754	1	transit
47	HAT-P-22 b	11.85	682.55	3.21	1248	0.92	5302	3	transit
48	WASP-13 b	15.44	158.95	4.35	1494	1.19	5989	1	transit
49	HAT-P-33 b	20.05	242.56	3.47	1799	1.40	6446	1	transit
50	TrES-4 A b	20.17	157.05	3.55	1644	1.45	6295	1	transit
51	WASP-82 b	18.33	394.20	2.71	2127	1.63	6490	1	transit
52	WASP-31 b	16.87	151.96	3.41	1502	1.16	6200	1	transit
53	HAT-P-45 b	15.65	283.57	3.13	1605	1.26	6330	2	transit
54	KELT-2A b	14.33	472.41	4.11	1671	1.31	6148	1	transit
55	WASP-26 b	14.06	326.81	2.76	1618	1.12	5950	2	occultation
56	TrES-2	12.83	398.34	2.47	1458	0.98	5850	4	transit
57	WASP-50 b	12.62	467.32	1.96	1354	0.89	5400	5	transit
58	WASP-63 b	15.69	120.80	4.38	1496	1.32	5570	1	transit
59	XO-2N b	10.68	189.79	2.62	1312	0.97	5332	2	transit
60	WASP-104 b	12.48	404.38	1.76	1476	1.08	5475	3	occultation
61	WASP-41 b	13.28	292.47	3.05	1278	0.95	5450	2	transit
62	HAT-P-40 b	18.98	195.51	4.46	1719	1.51	6080	1	transit
63	WASP-48 b	18.33	311.55	2.14	1980	1.19	5920	1	occultation
64	HAT-P-4 b	13.94	216.18	3.06	1653	1.26	5890	2	transit
65	WASP-4 b	14.96	356.53	1.34	1818	0.93	5500	1	occultation
66	WASP-103 b	17.59	467.32	0.93	2430	1.20	6110	1	occultation
67	WASP-75 b	13.94	340.16	2.48	1660	1.14	6100	2	occultation
68	Qatar-1 b	12.77	422.82	1.42	1347	0.85	4910	5	occultation
69	WASP-20 b	16.00	99.50	4.90	1345	1.20	5950	1	transit
70	TrES-3 b	14.32	607.20	1.31	1654	0.88	5720	1	occultation
71	PTFO 8-8695 b	20.96	953.72	0.45	1884	0.34	3470	1	occultation
72	HAT-P-1 b	13.35	166.58	4.47	1259	1.13	5975	1	transit
73	WASP-90 b	17.89	200.28	3.92	1791	1.55	6430	2	transit
74	HAT-P-46 b	14.09	156.73	4.47	1413	1.28	6120	1	transit
75	WASP-111 b	15.82	581.77	2.31	2065	1.50	6400	1	occultation

Table 6 (continued)

#	Planet	Planetary properties				Stellar properties		Observation	
		R (R_{\oplus})	M (M_{\oplus})	P (days)	T (K)	R (R_{\odot})	T (K)	#	Type
76	XO-1 b	12.99	286.12	3.94	1216	1.00	5940	1	transit
77	WASP-34 b	13.39	187.57	4.32	1131	1.01	5700	1	transit
78	WASP-88 b	18.65	178.03	4.95	1716	1.45	6431	1	transit
79	HATS-3 b	18.62	361.78	3.55	1757	1.30	6351	2	occultation
80	WASP-100 b	18.54	645.35	2.85	2143	1.57	6900	1	occultation
81	WASP-68 b	13.61	302.01	5.08	1447	1.24	5911	2	transit
82	CoRoT-2 b	16.08	1052.27	1.74	1484	0.97	5575	1	occultation
83	HAT-P-49 b	15.51	549.98	2.69	2072	1.54	6820	1	occultation
84	HAT-P-56 b	16.09	693.04	2.79	1791	1.30	6566	1	occultation
85	HAT-P-7 b	16.01	543.30	2.20	2141	1.59	6310	1	occultation
86	WASP-21 b	12.75	87.74	4.32	1298	0.89	5800	1	transit
87	WASP-22 b	12.71	186.93	3.53	1383	1.10	6000	2	transit
88	WASP-24 b	12.11	328.08	2.34	1611	1.13	6075	4	occultation
89	WASP-25 b	13.83	184.39	3.76	1209	1.00	5750	1	transit
90	HAT-P-5 b	13.74	336.98	2.79	1477	1.16	5960	6	transit
91	WASP-69 b	11.60	82.66	3.87	938	0.83	4715	1	transit
92	WASP-87 b	15.20	693.04	1.68	2251	1.20	6450	1	occultation
93	HAT-P-24 b	13.63	217.77	3.36	1581	1.19	6329	4	transit
94	HAT-P-39 b	17.24	190.43	3.54	1705	1.40	6430	3	transit
95	WASP-16 b	11.06	271.81	3.12	1235	1.02	5550	4	transit
96	TrES-1 b	12.06	241.93	3.03	1147	0.88	5250	2	transit
97	WASP-64 b	13.95	404.06	1.57	1587	0.98	5400	3	occultation
98	WASP-6 b	13.43	159.91	3.36	1161	0.89	5450	1	transit
99	WASP-55 b	14.27	181.21	4.47	1236	1.01	5900	1	transit
100	HAT-P-36 b	13.87	582.41	1.33	1778	1.02	5580	1	occultation
101	HAT-P-9 b	15.36	213.00	3.92	1490	1.28	6350	4	transit
102	HAT-P-14 b	13.17	699.40	4.63	1525	1.39	6600	3	occultation
103	WASP-28 b	13.31	288.34	3.41	1429	1.02	6150	6	transit
104	XO-4 b	14.70	546.80	4.13	1418	1.32	5700	6	occultation
105	WASP-58 b	15.03	282.94	5.02	1242	0.94	5800	2	transit
106	HAT-P-23 b	15.01	664.43	1.21	1997	1.13	5905	1	occultation
107	Qatar-2 b	12.55	790.63	1.34	1256	0.74	4645	9	occultation
108	WASP-5 b	12.85	520.41	1.63	1693	1.00	5700	2	occultation
109	WASP-65 b	12.20	492.76	2.31	1446	0.93	5600	7	occultation
110	CoRoT-1 b	16.35	327.44	1.51	1839	0.95	6298	1	occultation
111	HAT-P-27 b	11.19	197.10	3.04	1161	0.92	5300	3	transit
112	KELT-6 b	12.95	140.51	7.85	1284	1.13	6272	1	transit
113	WASP-45 b	12.73	320.13	3.13	1165	0.91	5140	6	transit

Table 6 (continued)

#	Planet	Planetary properties				Stellar properties		Observation	
		R (R_{\oplus})	M (M_{\oplus})	P (days)	T (K)	R (R_{\odot})	T (K)	#	Type
114	WASP-72 b	11.08	448.25	2.22	1819	1.23	6250	2	occultation
115	HATS-1 b	14.29	589.72	3.45	1332	0.99	5870	14	transit
116	WASP-78 b	19.20	368.77	2.18	2136	2.02	6100	1	occultation
117	WASP-96 b	13.17	152.60	3.43	1251	1.06	5540	3	transit
118	HAT-P-28 b	13.30	199.01	3.26	1345	1.02	5680	6	transit
119	WASP-39 b	13.94	89.01	4.06	1088	0.93	5400	1	transit
120	WASP-80 b	10.45	176.12	3.07	794	0.57	4145	1	transit
121	HATS-2 b	12.82	427.58	1.35	1528	0.88	5227	5	occultation
122	WASP-71 b	16.02	712.75	2.90	1987	1.56	6050	1	occultation
123	WASP-38 b	11.96	861.53	6.87	1218	1.23	6150	10	transit
124	WASP-110 b	13.58	162.13	3.78	1113	0.89	5400	1	transit
125	HAT-P-3 b	9.07	187.88	2.90	1115	0.92	5224	4	transit
126	WASP-47 b	12.84	336.98	4.16	1240	1.04	5576	8	transit
127	WASP-98 b	12.07	263.86	2.96	1149	0.69	5525	8	transit
128	WASP-46 b	14.38	667.92	1.43	1615	0.96	5620	3	occultation
129	HAT-P-25 b	13.06	180.22	3.65	1172	1.01	5500	3	transit
130	WASP-18 b	12.78	3315.77	0.94	2345	1.24	6400	1	occultation
131	WASP-67 b	15.36	133.52	4.61	1000	0.87	5200	1	transit
132	WASP-14 b	14.06	2333.75	2.24	1834	1.21	6462	1	occultation
133	WASP-60 b	9.44	163.40	4.31	1261	0.51	5900	6	transit
134	WASP-11 b	11.47	146.24	3.72	1002	0.82	4974	1	transit
135	HAT-P-35 b	14.62	335.07	3.65	1537	1.24	6096	12	occultation
136	WASP-36 b	13.93	724.51	1.54	1655	1.02	5881	3	occultation
137	HAT-P-50 b	14.13	429.17	3.12	1805	1.27	6280	3	occultation
138	WASP-99 b	12.07	883.78	5.75	1438	1.48	6180	6	occultation
139	HAT-P-42 b	14.01	309.96	4.64	1389	1.18	5743	13	transit
140	WASP-73 b	12.73	597.66	4.09	1736	1.34	6036	3	occultation
141	WASP-135 b	14.27	604.02	1.40	1673	0.98	5675	3	occultation
142	WASP-23 b	10.56	281.03	2.94	1099	0.78	5150	10	transit
143	TrES-5 b	13.27	565.24	1.48	1433	0.88	5171	10	occultation
144	HAT-P-16 b	13.06	1332.98	2.78	1527	1.22	6140	3	occultation
145	Kepler-12 b	19.20	136.70	4.44	1341	1.09	5953	2	transit
146	Kepler-7 b	17.71	137.65	4.89	1584	1.36	5933	4	transit
147	WASP-44 b	11.00	276.26	2.42	1275	0.92	5410	28	transit
148	XO-5 b	11.30	342.39	4.19	1206	0.88	5510	16	transit
149	HAT-P-43 b	14.08	209.82	3.33	1322	1.05	5645	12	transit
150	HAT-P-55 b	12.97	185.02	3.58	1278	1.01	5808	10	transit
151	WASP-32 b	13.06	1144.46	2.72	1507	1.10	6100	5	occultation

Table 6 (continued)

#	Planet	Planetary properties				Stellar properties		Observation	
		R (R_{\oplus})	M (M_{\oplus})	P (days)	T (K)	R (R_{\odot})	T (K)	#	Type
152	HAT-P-29 b	12.15	247.33	5.72	1224	1.21	6087	8	transit
153	WASP-10 b	11.85	972.79	3.09	1009	0.71	4675	37	transit
154	Kepler-6 b	14.27	213.00	3.23	1354	1.05	5640	15	transit
155	HD219134b	1.61	4.47	3.09	934	0.78	4699	1	transit
156	HATS-13 b	13.30	172.62	3.04	1212	0.96	5523	10	transit
157	HAT-P-51 b	14.19	98.23	4.22	1159	0.98	5449	2	transit
158	HAT-P-34 b	13.14	1057.99	5.45	1440	1.39	6442	10	occultation
159	WASP-37 b	12.47	539.17	3.58	1293	0.85	5800	43	transit
160	WASP-56 b	11.98	181.52	4.62	1117	1.03	5600	4	transit
161	WASP-66 b	15.25	737.54	4.09	1754	1.30	6600	3	occultation
162	WASP-112 b	13.07	279.76	3.04	1349	0.81	5610	28	transit
163	HAT-P-44 b	14.05	124.62	4.30	1092	0.94	5295	2	transit
164	HAT-P-37 b	12.93	371.63	2.80	1166	0.93	5500	37	transit
165	Gliese 436 b	4.13	23.11	2.64	695	0.45	3684	1	transit
166	WASP-29 b	8.69	77.57	3.92	970	0.82	4800	1	transit
167	HD 219134 b	1.57	3.81	3.09	931	0.79	4699	1	transit
168	HAT-P-12 b	10.52	67.08	3.21	932	0.73	4650	1	transit
169	Kepler-13 A b	15.43	2571.87	1.76	2389	1.72	7200	1	occultation
170	HAT-P-19 b	12.17	92.83	4.01	982	0.84	4990	1	transit
171	CoRoT-11 b	15.25	791.59	2.99	1686	1.27	6440	5	occultation
172	Kepler-8 b	15.58	187.57	3.52	1528	1.13	6251	20	transit
173	HATS-10 b	10.63	167.22	3.31	1369	1.10	5880	28	transit
174	WTS-2 b	14.96	356.06	1.02	1495	0.82	5000	16	occultation
175	HAT-P-52 b	11.07	260.05	2.75	1184	0.89	5131	43	transit
176	HAT-P-20 b	9.51	2303.55	2.88	946	0.76	4595	97	occultation
177	WASP-120 b	16.62	1592.71	3.61	1842	1.45	6450	1	occultation
178	HATS-9 b	11.69	266.09	1.92	1769	1.03	5366	9	occultation
179	CoRoT-19 b	15.91	352.88	3.90	1616	1.21	6090	16	occultation
180	OGLE-TR-10 b	18.87	216.18	3.10	1554	1.28	6075	16	occultation
181	WASP-42 b	11.85	158.95	4.98	969	0.88	5200	1	transit
182	WASP-61 b	13.61	654.89	3.86	1509	1.22	6250	17	occultation
183	HAT-P-31 b	11.74	690.18	5.01	1343	1.22	6065	43	occultation
184	HAT-P-53 b	14.46	471.77	1.96	1624	1.09	5956	7	occultation
185	WASP-8 b	11.39	713.38	8.16	906	1.03	5600	6	transit
186	HATS-4 b	11.19	420.59	2.52	1282	1.00	5403	97	occultation
187	Kepler-447 b	18.11	435.53	7.79	908	0.76	5493	2	transit
188	Kepler-76 b	14.92	638.99	1.54	2074	1.20	6409	2	occultation
189	WASP-57 b	10.05	213.63	2.84	1430	1.01	5600	43	occultation

Table 6 (continued)

#	Planet	Planetary properties				Stellar properties		Observation	
		R (R_{\oplus})	M (M_{\oplus})	P (days)	T (K)	R (R_{\odot})	T (K)	#	Tpe
190	CoRoT-5 b	15.23	148.46	4.04	1315	1.00	6100	15	transit
191	HD 17156 b	12.02	1014.44	21.22	816	1.27	6079	9	transit
192	Kepler-412 b	14.54	298.51	1.72	1780	1.17	5750	12	occultation
193	XO-3 b	13.35	3748.12	3.19	1665	1.21	6429	1	occultation
194	WASP-117 b	11.20	87.58	10.02	997	1.13	6040	1	transit
195	Gliese 1214 b	2.77	6.20	1.58	552	0.18	3250	1	transit
196	Gliese 3470 b	3.80	13.73	3.34	635	0.51	3652	1	transit
197	HAT-P-11 b	4.96	25.75	4.89	848	0.81	4780	1	transit
198	GJ 1132 b	1.16	1.62	1.63	529	0.18	3270	1	transit
199	Gliese 436 c	0.66	0.28	1.37	813	0.45	3684	1	transit
200	HAT-P-26 b	6.20	18.76	4.23	967	0.82	5079	1	transit
201	HAT-P-18 b	10.39	62.31	5.51	818	0.77	4870	1	transit
202	HD 97658 b	2.34	7.55	9.49	729	0.77	5119	1	transit
203	HAT-P-17 b	11.08	169.76	10.34	758	0.86	5246	1	transit
204	WASP-84 b	10.70	222.53	8.52	780	0.85	5280	1	transit
205	HATS-6 b	10.95	101.41	3.33	693	0.57	3724	1	transit
206	EPIC 203771098 c	7.93	27.02	42.36	596	1.12	5743	1	transit
207	KOI-142 b	4.13	1.76	10.95	764	1.02	5513	1	transit
208	HATS-5 b	10.01	75.34	4.76	998	0.94	5304	1	transit
209	Kepler-51 b	6.95	2.10	45.15	496	1.04	6018	1	transit
210	HAT-P-2 b	10.44	2778.51	5.63	1443	1.36	6290	1	occultation

References

1. Baraffe, I., Chabrier, G., Allard, F., Hauschildt, P.H.: Evolutionary models for solar metallicity low-mass stars: mass-magnitude relationships and color-magnitude diagrams. *A&A* **337**, 403–412 (1998)
2. Casagrande, L., Schönrich, R., Asplund, M., Cassisi, S., Ramírez, I., Meléndez, J., Bensby, T., Feltzing, S.: New constraints on the chemical evolution of the solar neighbourhood and Galactic disc(s). Improved astrophysical parameters for the Geneva-Copenhagen Survey. *A&A* **530**, A138 (2011)
3. Chen, J., Kipping, D.M.: Probabilistic forecasting of the masses and radii of other worlds. *apj* **834**, 17 (2017). <https://doi.org/10.3847/1538-4357/834/1/17>
4. Cohen, M., Wheaton, W.A., Megeath, S.T.: Spectral irradiance calibration in the infrared. XIV. The absolute calibration of 2MASS. *AJ* **126**, 1090–1096 (2003)
5. Fressin, F., Torres, G., Charbonneau, D., Bryson, S.T., Christiansen, J., Dressing, C.D., Jenkins, J.M., Walkowicz, L.M., Batalha, N.M.: The false positive rate of kepler and the occurrence of planets. *ApJ* **766**, 81 (2013)
6. Fulton, B.J., Petigura, E.A., Howard, A.W., Isaacson, H., Marcy, G.W., Cargile, P.A., Hebb, L., Weiss, L.M., Johnson, J.A., Morton, T.D., Sinukoff, E., Crossfield, I.J.M., Hirsch, L.A.: The California-Kepler survey. III. A gap in the radius distribution of small planets. *aj* **154**, 109 (2017). <https://doi.org/10.3847/1538-3881/aa80eb>
7. Mayo, A.W., Vanderburg, A., Latham, D.W., Bieryla, A., Morton, T.D., Buchhave, L.A., Dressing, C.D., Beichman, C., Berlind, P., Calkins, M.L., Ciardi, D.R., Crossfield, I.J.M., Esquerdo, G.A.,

- Everett, M.E., Gonzales, E.J., Hirsch, L.A., Horch, E.P., Howard, A.W., Howell, S.B., Livingston, J., Patel, R., Petigura, E.A., Schlieder, J.E., Scott, N.J., Schumer, C.F., Sinukoff, E., Teske, J., Winters, J.G.: 275 candidates and 149 validated planets orbiting bright stars in K2 campaigns 0–10. ArXiv e-prints arXiv:1802.05277 (2018)
8. Mulders, G.D., Pascucci, I., Apai, D.: An increase in the mass of planetary systems around lower-mass stars. *ApJ* **814**, 130 (2015)
 9. Mulders, G.D., Pascucci, I., Apai, D., Frasca, A., Molenda-Zakowicz, J.: A super-solar metallicity for stars with hot rocky exoplanets. *aj* **152**, 187 (2016). <https://doi.org/10.3847/0004-6256/152/6/187>
 10. Öberg, K.I., Boogert, A.C.A., Pontoppidan, K.M., van den Broek, S., van Dishoeck, E.F., Bottinelli, S., Blake, G.A., Evans, N.J.I.I.: The spitzer ice legacy: ice evolution from cores to protostars. *ApJ* **740**, 109 (2011)
 11. Pascale, E., Waldmann, I.P., MacTavish, C.J., Papageorgiou, A., Amaral-Rogers, A., Varley, R., Coudé du Foresto, V., Griffin, M.J., Ollivier, M., Sarkar, S., Spencer, L., Swinyard, B.M., Tessenyi, M., Tinetti, G.: ECHOSim: the Exoplanet Characterisation Observatory software simulator. *Exp. Astron.* **40**, 601–619 (2015)
 12. Piskorz, D., Knutson, H.A., Ngo, H., Muirhead, P.S., Batygin, K., Crepp, J.R., Hinkley, S., Morton, T.D.: Friends of hot Jupiters. III. an infrared spectroscopic search for low-mass stellar companions. *ApJ* **814**, 148 (2015)
 13. Puig, L., Isaak, K., Linder, M., Escudero, I., Crouzet, P.-E., Walker, R., Ehle, M., Hübner, J., Timm, R., de Vogeleer, B., Drossart, P., Hartogh, P., Lovis, C., Micela, G., Ollivier, M., Ribas, I., Snellen, I., Swinyard, B., Tinetti, G., Eccleston, P.: The phase 0/A study of the ESA M3 mission candidate EChO. *Exp. Astron.* **40**, 393–425 (2015)
 14. Ribas, I., Lovis, C.: Echo targets: the mission reference sample and beyond [EChO-SRE-SA-PhaseA-001_MRSv2.4], european space agency (2013)
 15. Sarkar, S., Papageorgiou, A., Pascale, E.: Exploring the potential of the ExoSim simulator for transit spectroscopy noise estimation. In: *Space telescopes and instrumentation 2016: optical, infrared, and millimeter wave*, vol. 9904, p. 99043R (2016)
 16. Sarkar, S., Pascale, E.: ExoSim: a novel simulator of exoplanet spectroscopic observations. European Planetary Science Congress 2015, held 27 September - 2 October, 2015 in Nantes, France, Online at (2015)
 17. Sullivan, P.W., Winn, J.N., Berta-Thompson, Z.K., Charbonneau, D., Deming, D., Dressing, C.D., Latham, D.W., Levine, A.M., McCullough, P.R., Morton, T., Ricker, G.R., Vanderspek, R., Woods, D.: The transiting exoplanet survey satellite: Simulations of planet detections and astrophysical false positives. *ApJ* **809**, 77 (2015)
 18. Triaud, A.H.M.J., Lanotte, A.A., Smalley, B., Gillon, M.: Colour-magnitude diagrams of transiting Exoplanets - II. a larger sample from photometric distances. *MNRAS* **444**, 711–728 (2014)
 19. Valencia, D., Sasselov, D.D., O’Connell, R.J.: Detailed models of super-earths: how well can we infer bulk properties? *ApJ* **665**, 1413–1420 (2007)
 20. Venot, O., Hébrard, E., Agúndez, M., Decin, L., Bounaceur, R.: New chemical scheme for studying carbon-rich exoplanet atmospheres. *A&A* **577**, A33 (2015)